4 Probabilistic Seismic Hazard Assessment of West Bengal with special emphasis on Kolkata

4.1 Introduction

Safe urbanization and earthquake disaster mitigation protocol necessitates seismic hazard assessment either by Probabilistic or Deterministic means for the generation of design response spectra at a site of interest with an appropriate zone factor for the computation of seismic coefficient to be adapted in building code. The State of West Bengal with over 91 million inhabitants is the fourth most populous states in India and seventh-most populous sub-national entity in the world. West Bengal is located in Bengal fan basin which has been predominantly considered as stable and of sparse seismicity. However occurrence of some devastating earthquakes *viz*. 1897 Great Shillong earthquake of M_w 8.1, 1950 Assam earthquake of M_w 8.7, 1930 Dhubri earthquake of M_w 7.1, 1934 Bihar-Nepal earthquake of M_w 8.1, 1964 Sagar Island earthquake of M_w 5.4, 2011 Sikkim earthquake of M_w 6.9 and the recent 2015 Nepal earthquake of M_w 7.8 within about 500 km circumscribing West Bengal has ample proof of seismic vulnerability in the region. The Shillong plateau, Eocene Hinge Zone and the Central Himalayan subduction zone are the principal source of seismicity in the region. The Bureau of Indian Standards (BIS, 2002) places West Bengal in Seismic Zones II–V, corresponding to peak ground acceleration (PGA) of the order of 0.1 to 0.36g. The lowest hazard Zone II is associated with the southwestern part of West Bengal while Zone III covers the central part of West Bengal. The districts of Kolkata, Murshidabad, Birbhum, Bardhaman, Hooghly, Howrah, Nadia, Bankura and East & West Medinipur come under Zone III. The Zone IV is delineated on the northern and parts of southeastern region. The northern portion encompassing Darjeeling, North and South Dinajpur, parts of Jalpaiguri and Cooch Behar, North and South 24-Parganas and Malda fall under Zone IV. Some portion of southeastern regions like Barasat also lies in Zone IV. Zone V is delineated on the eastern parts of Cooch Behar and Jalpaiguri region. The Bengal Basin has considerable area close to river basins and deltas that are characterized by Holocene alluvium deposits, which are likely to soften and hence are susceptible to liquefaction during large and great earthquake as

is reported in GSI memoir (1939) due to the impending of 1934 Bihar-Nepal earthquake of M_w 8.1. Thus the State of West Bengal can be considered mostly seismic vulnerable region. The damage pattern due to an earthquake depends largely on the local site condition and the social infrastructure of the region with the most important condition being the intensity of ground shaking due to the impending of an earthquake. Contrasting seismic response is observed even within a short distance over small changes in geology. The challenge of urban hazard mapping is to predict the ground motion effects related to various source, path and site characteristics with an acceptable level of reliability. The state capital Kolkata is placed on a sedimentary deposit having a thickness of the order of 7.5 km above the crystalline basement and has developed primarily along the eastern bank of the River Hooghly during the last 300+ years and is considered one of the most densely populated cities in the world needing special attention towards site-specific seismic hazard in the region for the purpose of earthquake inflicted disaster mitigation and management. The 1934 Bihar-Nepal earthquake of M_w 8.1 inflicted considerable damage to life and property in Kolkata (GSI, 1939) adhering to MM intensity of VI-VII. The near source earthquakes reported in Kolkata include the 1906 Kolkata earthquake with MM intensity V-VI (Middlemiss, 1908), 1885 Bengal earthquake of M_w 6.8 with MM intensity V (Martin and Szeliga, 2010), 1935 Pabna earthquake of M_w 6.2 with MM intensity V (Martin and Szeliga, 2010) and 1964 Sagar Island earthquake of M_w 5.4 with damage intensity of MM VI-VII surrounding the Kolkata city (Nath *et al*., 2014). The prevailing seismic zoning map of India (BIS, 2002) prepared based on the Peak Ground Acceleration (PGA) induced by the Maximum Considered Earthquake (MCE) further constrained by the geologic and seismotectonic considerations thus scaling down to the Design Basis Earthquake (DBE) for urban codal provisions, places the entire city of Kolkata at the boundary between Zone III and IV with an equivalent PGA range of 0.16-0.24g. Thus, the Seismic Hazard framework encompassing the seismicity, seismic sources, and earthquake potential based on available historical & instrumental data covering hundreds of years, micro- and macro-seismicity, regional tectonics & neo-tectonics (faults/ lineaments), geology, geo-hydrology, crustal structure, sub-surface lithostratigraphy is crucial and mandatory to alleviate quake catastrophe for the successful implementation of safety regulations.

In order to develop effective earthquake measures it is, therefore, necessary that the seismic hazard associated with the earthquakes are realistically estimated for the terrain. An attempt has been made to generate an updated seismic hazard scenario of West Bengal and Kolkata by employing new data, recent findings, and the adaptation of improved methodology. Thus, in the present study Probabilistic Seismic Hazard analysis has been carried out to deliver an updated seismic hazard map of West Bengal and also of Kolkata in 1:25,000 scale in terms of Peak Ground Acceleration (PGA) and Pseudo Spectral Acceleration (PSA) for different time periods at firm rock site conditions adopting a protocol as depicted in Figure 4.1.

In computing Probabilistic Seismic Hazard, we include two different earthquake source models: Layered Polygonal seismic sources and Tectonic sources. The spatial variation of seismicity parameters *i.e. b-value* is ascertained along with the prognosis of Maximum Credible

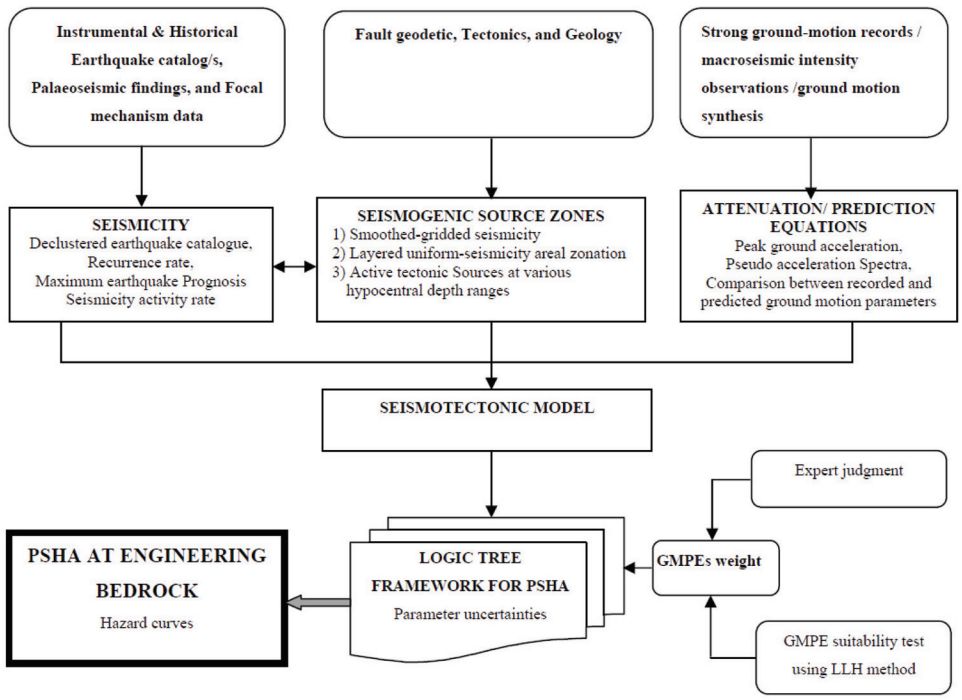

Figure 4.1 **Key components and workflow of Probabilistic Seismic Hazard Assessment (Maiti *et al.*, 2015).**

Earthquake (M_{max}). Smoothening seismicity has been performed in order to understand the activity rate of earthquake occurrence for both the Layered Polygonal and the Tectonic sources. Due to the unavailability of well-established attenuation relations for the region, six new Next Generation Attenuation models (NGA) have been developed by nonlinear regression analysis for the three tectonic provinces namely the East Central Himalaya, Northeast India and the Bengal Basin itself. The models given by Atkinson and Boore (2006) and Campbell and Bozorgnia (2003) have been used as fundamental equations for the generation of NGA models for this region. Besides the new prediction models developed in the present study both the regional and the global attenuation models reported for the same region or in the regions with similar tectonic setup have been utilized in the hazard computation for both West Bengal and its capital city, Kolkata. Eventually all the hazard contributing components *viz*. source attribution, seismic activity rates, Ground motion prediction equations (GMPE) are judiciously integrated with appropriate weights and ranks in a logic tree framework to deliver PGA and 5% damped PSA distributions with 10% and 2% probability of exceedance in 50 years.

4.2 Methodology

4.2.1 Seismogenic Source Definition in the Region

A successful seismogenic source definition requires a declustered homogeneous earthquake catalog of the study region. We, therefore, prepared an earthquake catalog of the Bengal Basin and the adjoining region spanning for a period of 1900-2014 by considering three major earthquake data sources, namely the International Seismological Centre (ISC, http://www.isc.ac.uk), U.S. Geological Survey/National Earthquake Information Center (USGS/ NEIC, http://neic.usgs.gov.us), and Global Centroid Moment Tensor (GCMT, http://www.globalcmt.org), wherein the hypocentral depth entries have been computed using the algorithm given by Engdahl *et al.* (1998). Other data sources used include India Meteorological Department (IMD, http://www.imd.ernet.in), and Jaiswal and Sinha (2004). For uniform magnitude scaling and establishing data homogeneity for meaningful statistical analysis M_w is preferred owing to its applicability for all ranges of earthquakes; large or small, far or near, shallow or deep-focused. Thereafter, the entire catalogue has been declustered to remove foreshocks and aftershocks to derive a mainshock catalogue accessible at http://www.earthqhaz.net/sacat/. The detailed homogeneous earthquake catalogue preparation is described in Chapter 3. The source characterization also includes the fault database which is compiled on Geographical Information System. The sources include seismotectonic map of India published by Geological Survey of India (Dasgupta *et al.,* 2000) and the one extracted from Landsat TM/MSS & SRTM data. To characterize the seismogenic sources responsible for significantly contributing to the seismic hazard of Bengal Basin, the earthquakes from the catalogue supplemented by records of historical earthquakes (occurring prior to 1900 and as early as A.D. 819) and instrumental data covering a period from 1900-2014 are projected with the fault pattern in the region. Thus in the present study we classified seismogenic sources based on two categories *viz*. (a) Layered Polygonal sources, and (b) Active Tectonic sources.

Practically it is difficult at times to establish definite tectonic class for a given zone. While, the source zonation becomes a case of tectonic dismantling, reduced seismogenic zone dimensions with sparse earthquake occurrences would obscure seismicity parameterization. In that respect, seismicity smoothening or zone-free approach is considered pragmatic to account for the absence of fault associability while adhering to the spatial distribution of earthquake occurrences. This complies with the fact that the locations of future large earthquakes tend to follow those of the past seismicity (Kafka, 2007; Parsons, 2008). The approach has been in vogue ever since the publication of the works of Vere-Jones (1992), Kagan and Jackson (1994), and Frankel (1995). Recent studies employed seismicity smoothing for small to moderate earthquakes and fault specific zonation for larger earthquakes (*e.g.* Petersen *et al.,* 2008; Kalkan *et al.*, 2009). Alternately, unified approach can be formulated such that seismicity models based on area zonation employed for the estimation of b-value and M_{max} prognosis while seismicity smoothing is used to establish the distribution of seismic activity rate. This delineates the grid cells according to regions of homogenous seismotectonic characteristics. Eventually, the methodology adopted in the present study can be outlined as: (1) delineation of areal source zones, (2) derivation of seismicity model for each zone, and (3) application of seismicity smoothening algorithm to obtain activity rates for specific threshold magnitudes.

4.2.1.1 Layered Polygonal Seismogenic Source Zones

A popular approach in the seismogenic localization process is the areal source zonation, wherein the objective is to capture uniform seismicity. The seismicity pattern and seismogenic source dynamics are known to have significant variations with depth (*e.g.* Prozorov and Dziewonski, 1982; Christova, 1992; Tsapanos, 2000; Allen *et al.,* 2004, Nath and Thingbaijam, 2012). This has also been considered by workers in other parts of the globe (*e.g.* Stirling *et al.*, 2002; Suckale and Grünthal, 2009). Hence, by considering single set of seismicity parameter over the entire depth range may lead to incorrect hazard estimation. In the Indian subcontinent previous studies have been carried out by Khattri *et al.* (1984) and Bhatia *et al.* (1999) to delineate seismogenic source zones. But it has been observed that consistent definition criteria have not been adopted across the entire territory. In the present context we found the methodology given by Nath and Thingbaijam (2012) is more appropriate and, therefore, it has been adopted here. In the present study based on seismicity variation with hypocentral depth, two depth ranges (in km) *viz*. 0-25 and 25-70 are considered. The source zonation is thereupon carried out based on the seismicity pattern, the fault network and the similarity in focal mechanism (*e.g.* Cáceres *et al.,* 2005) thus demarcating 33 source zones as depicted in Figure 4.2. The layered model approach is expected to facilitate source characterization more precisely than the conventional single layer schemes hitherto considered by other workers.

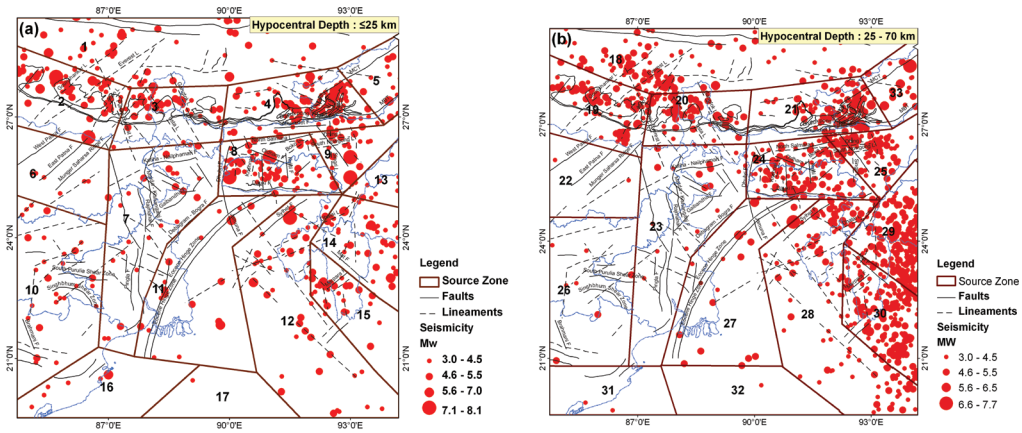

Figure 4.2 **A layered polygonal seismogenic source framework at the hypocentral depth ranges (a) 0-25 km, and (b) 25-70 km for West Bengal and its adjoining region as modified after Nath and Thingbaijam (2012) for PSHA.**

4.2.1.2 Active Tectonic Seismogenic Source Zones

Additional seismogenic sources considered are the active tectonic features such as the faults and lineaments (Azzaro *et al.,* 1998; Slemmons and McKinney, 1977). As discussed earlier, the Bengal Basin encompasses many active faults and lineaments which can be considered potential sources contributing to seismic hazard of the region. Fault based source consideration has never been used in most of the previous studies by Khattri *et al.* (1984), Bhatia *et al.* (1999), Jaiswal and Sinha

(2007), Nath and Thingbaijam (2012), and Sitharam and Kolathayar (2013) for PSHA. In the present study, active tectonic features are extracted from the seismotectonic atlas of India (Dasgupta *et al.*, 2000) and additional features by image processing of Landsat^{TM} data (http://glovis.usgs.gov/). The neo-tectonic features (faults and lineaments) have been identified and extracted from Landsat TM/MSS and SRTM data. Emphasis has also been given to large-scale lineaments that might have relevance to geomorphology, tectonic contact zones, aligned vegetation patterns, abrupt drainage patterns/river which are generally related to faults. For this purpose, all the lineaments were traced using the edge enhancement filters and principal component analysis. The available tectonic information from ISRO's '*Bhuvan*' website has also been used to extract the structural lineaments. The earthquake seismicity occurrences were linked to all possible active faults/lineaments which were not identified earlier but have the potential of generating significant earthquakes in the region. The focal mechanism data employed in the present study are derived from Global Centroid Moment Tensor (GCMT, www.globalcmt.org) database covering the period from 1976 to 2014 and other reportings of Dasgupta *et al.* (2000), Chandra (1977), Singh and Gupta (1980) and Bilham and England (2001). In total we have identified 158 active tectonic features (*i.e.* faults and lineaments) in the 0-25 km and 25-70 km depth ranges which expectedly have the potential of generating earthquakes of M_w 3.5 and above. Figure 4.3 depicts the major active tectonic sources of West Bengal and its adjoining region.

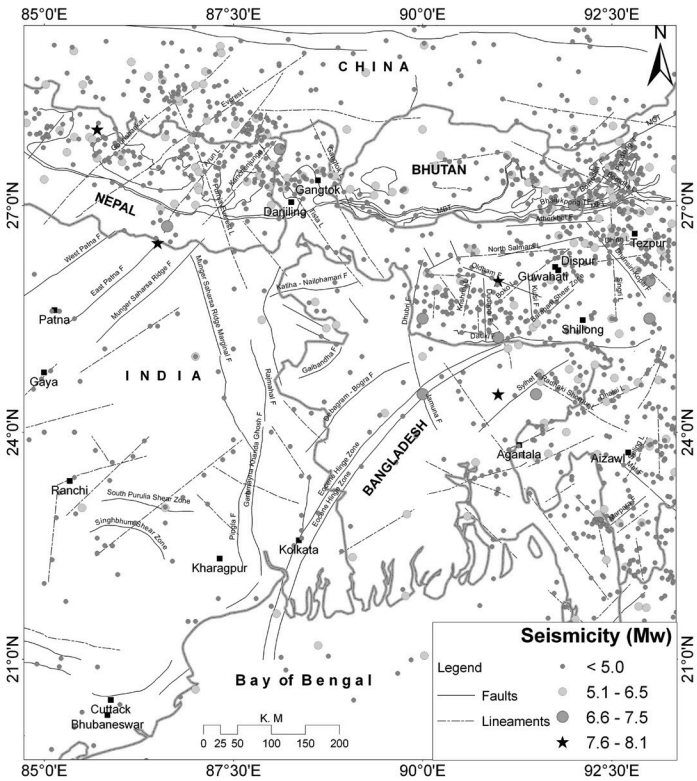

Figure 4.3 **Major active tectonic sources of West Bengal and its adjoining region.**

4.2.2 Maximum Earthquake Prognosis

The maximum earthquake (M_{max}), is the largest seismic event characteristic of a terrain with well-defined tectono-stratigraphic settings. The M_{max} values are often calculated from fault dimensions and geodetic inferences (Wells and Coppersmith, 1994; Anderson *et al.,* 1996), in addition to the frequency magnitude distribution obtained from past seismicity. Maximum earthquake prognosis has been performed for both the layered polygonal sources and the active tectonic sources. For polygonal sources a maximum likelihood method referred to as Kijko-Sellevoll-Bayesian (Kijko, 2004; Kijko and Graham, 1998) has been used. The technique is based on Bayesian equation of frequency magnitude distribution. It has been observed that empirical magnitude distribution deviates moderately from the Gutenberg-Richter relation following an exponential tail of a Gamma function at larger magnitudes. A computer program available for M_{max} estimation as given by Kijko (2004) has been employed in the present study.

The deterministic assessment of characteristic earthquake *viz*. maximum earthquakes from a fault is generally achieved with a relationship between earthquake magnitude and co-seismic sub-surface fault rupture length. The primary method used to estimate subsurface rupture length and rupture area is the spatial pattern of early aftershocks (Wells and Coppersmith, 1994). Aftershocks that occur within a few hours to a few days of the mainshock generally define the maximum extent of co-seismic fault rupture (Kanamori and Anderson, 1975; Dietz and Ellsworth, 1990; Wong *et al.,* 2000). Basically, an aftershock zone roughly corresponds to fault rupture during the mainshock, but precise studies indicate that aftershocks are concentrated near the margin of the fault area where the large displacement occurred (*e.g.* Das and Henry, 2003; Utsu, 2002). The general assumption, based on worldwide data, is that 1/3 to 1/2 of the total length of fault would rupture when it generates the maximum earthquake (Mark, 1977; Kayabalia and Akin, 2003; Shukla and Choudhury, 2012; Seyrek and Tosun, 2011). In the present study, the fault rupture segmentation have been identified using the maximum length of the well-defined mainshock and aftershock zone along the faults (Besana and Ando, 2005; Utsu, 2002; Wells and Coppersmith, 1994), thereafter a GIS based onscreen digitization method have been used for the estimation of subsurface rupture length of each active tectonic feature. The Maximum Credible Earthquake has been estimated using the relationship given by Wells and Coppersmith (1994) based on subsurface fault rupture dimension and magnitude. Table 4.1 enlists some major active tectonic sources, their total length (TFL), the associated observed maximum earthquakes ($Mmax_{obs}$), the subsurface rupture length (RLD) and the maximum predicted earthquake (M_{max}).

Table 4.1 **Some major active tectonic features with total fault length (TFL), observed maximum earthquake ($Mmax_{obs}$), subsurface rupture length (RLD), and the estimated maximum earthquake (M_{max}) in West Bengal and its adjoining region**

Fault Name	TFL (km)	$Mmax_{obs}$	Fault Type	RLD (km)	M_{max}
Pyudung Thrust Fault	172	5.1	Reverse	46	7.0(±0.26)
Main Boundary Thrust	725	6.6	Reverse	74	7.3(±0.26)
Dhubri Fault	248	7.1	Reverse	175	7.8(±0.26)

Fault Name	TFL (km)	$Mmax_{obs}$	Fault Type	RLD (km)	M_{max}
Atherkhet Fault	143	5.2	Strike-slip	20	6.3(±0.24)
Dhansiri-Kopili Fault	142	4.8	Strike-slip	25	6.4(±0.24)
Bomodila Fault	83	4.9	Reverse	34	6.8(±0.26)
Kalaktang Fault	105	5.2	Reverse	18	6.4(±0.26)
Sylhet Fault	234	7.6	Strike-slip	198	7.8(±0.24)
Pyudung Fault	142	5.6	Reverse	24	6.5(±0.26)
Main Central Thrust	468	6.5	Reverse	123	7.6(±0.26)
Main Frontal Thrust	103	5.3	Reverse	23	6.5(±0.26)
Eocene Hinge	608	6.2	Strike-slip	47	6.8(±0.24)
Dauki Fault	342	7.1	Strike-slip	110	7.4(±0.24)
Everest Lineament	324	5.2	Strike-slip	35	6.6(±0.24)
Gourishankar Lineament	293	5.6	Strike-slip	63	7.0(±0.24)
Tista Lineament	257	5.5	Strike-slip	70	7.1(±0.24)
Gangtok Lineament	44	5	Strike-slip	19	6.2(±0.24)
Arun Lineament	265	6.8	Oblique Reverse	65	7.2(±0.26)
Himalayan Frontal Thrust	387	8.1	Reverse	335	8.3(±0.26)
Krishnai Lineament	80	4.9	Strike-slip	17	6.1(±0.24)
Jangipur-Gaibanda Fault	48	4.1	Strike-slip	4.9	5.3(±0.24)
Jamuna Fault	124	6.8	Strike-slip	80	7.2(±0.24)

4.2.3 Seismicity Parameters

The evaluation of seismicity parameters is one of the most important steps in the hazard estimation. Earthquake occurrences across the globe follow the Gutenberg and Richter (GR) relationship

$$\log_{10}\lambda(m) = a - bm \tag{4.1}$$

where, $\lambda(m)$ is the cumulative number of events with magnitude $\geq m$ (Gutenberg and Richter, 1944). The slope parameter, commonly termed *b-value*, is often employed as an indicator of stress regime in the tectonic reinforcements, and to characterize seismogenic zones (Schorlemmer *et al.*, 2005). The maximum likelihood method for the estimation of *b-value* given by Aki (1965) and Utsu (1965) can be written as

$$b = \frac{\log_{10}(e)}{\left[m_{mean} - (m_t - \frac{\Delta m}{2})\right]} \tag{4.2}$$

where, m_{mean} is the average magnitude, m_t is the minimum magnitude of completeness, and Δm is the magnitude bin size (= 0.1 in the present study). The standard deviation of *b-value* (δb) has been computed by the bootstrapping method as suggested by Schorlemmer *et al.* (2003) which involves repeated computations, each time employing redundant data sample, allowing events drawn from the catalog to be selected more than once. A minimum magnitude constraint is generally applied on the GR relation given by equation (4.1) on the basis of the magnitude of completeness entailed by the linearity of the GR relation on the lower magnitude range. An upper magnitude has been suggested in accordance with the physical dissipation of energy and the constraints due to the tectonic framework (Kijko, 2004). This is achieved by establishing the maximum earthquake M_{max} physically capable of occurring within a defined seismic regime in an underlying tectonic setup. The magnitude distribution is, therefore, truncated at M_{max} such that $M_{max} >> m_{min}$. A modified version of equation (4.1) formulated by Page (1968) and Cornell and Vanmarcke (1969) is a truncated exponential distribution (TGR) as follows

$$\lambda(m) = \lambda(m_{\min}) \frac{10^{-b(m-m_{\min})} - 10^{-b(M_{\max}-m_{\min})}}{1-10^{-b(M_{\max}-m_{\min})}} \tag{4.3}$$

where, m_{min} is the minimum magnitude, M_{max} is an upper-bound magnitude. The maximum earthquake (M_{max}), is the largest seismic event characteristic of the terrain under the tectono-stratigraphic consideration. The *b-value* and *a-value* are estimated by applying the maximum likelihood method (Aki, 1965; Utsu, 1965) on the instrumental catalog. The incomplete data (including the historical data) are rendered return periods according to the models, namely Gutenberg-Richter (GR) and Truncated Gutenberg-Richter (TGR) models. The linear GR relation can statistically accommodate large events if the seismic source zone is of appropriate size and the temporal coverage of the catalog is also long enough, TGR model is reckoned to be more appropriate considering the energy dissipations at larger magnitudes. In several cases, zones with similar tectonics are merged to achieve sufficient number of events say ≥50 in the present case as well as an acceptable uncertainty with the estimated seismicity parameters. This ultimately produced 21 zones out of a total of 33 zones. Seismicity analysis have been performed in these zones to estimate both the *a-* and *b- values*. Frequency magnitude distribution plots for main-shock events in each of the seismogenic source zones are depicted in Figure 4.4. The seismicity parameters estimated for all the polygonal seismogenic sources are listed in Table 4.2.

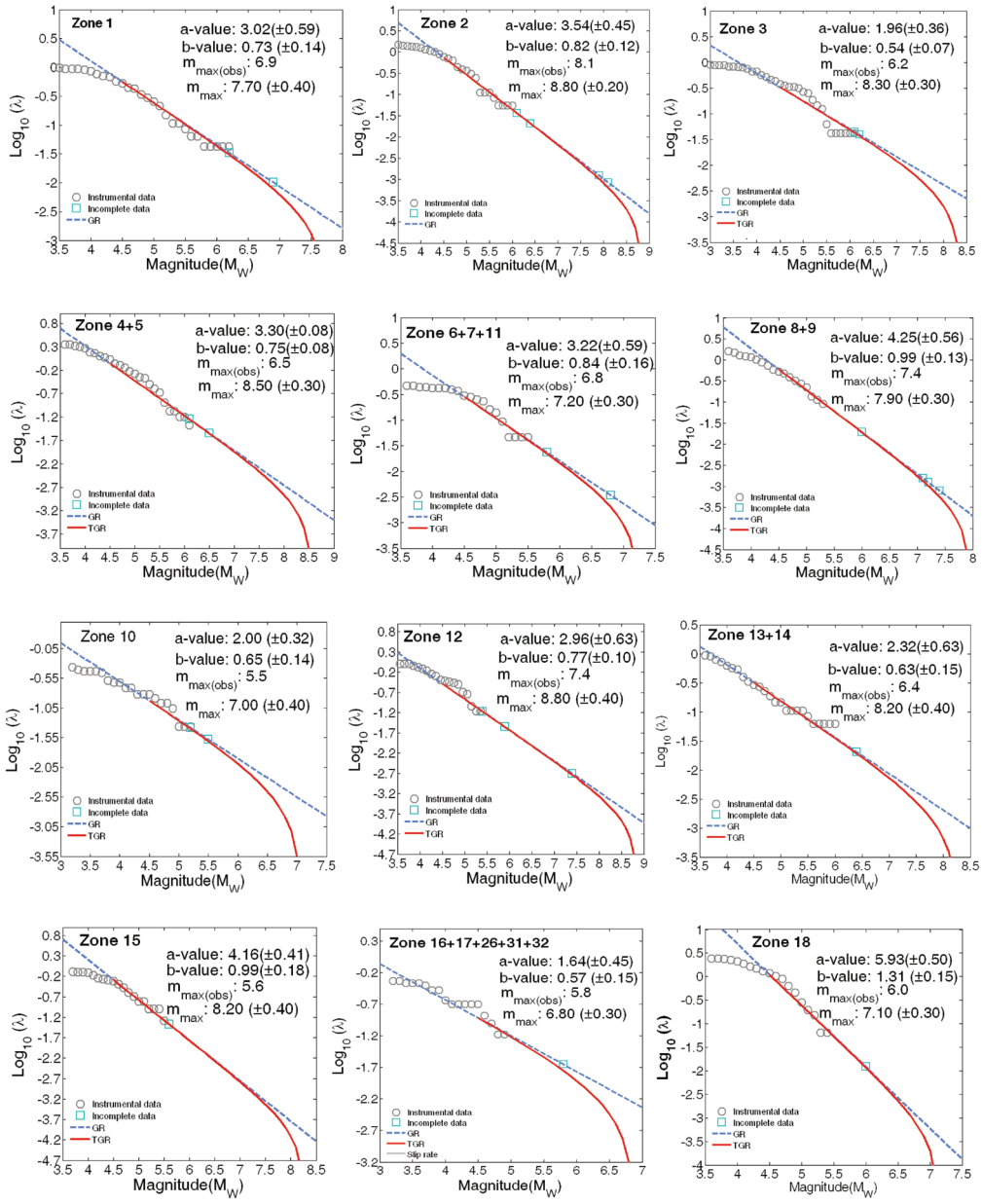
Zone 1
a-value: 3.02(±0.59)
b-value: 0.73 (±0.14)
m max(obs): 6.9
m max: 7.70 (±0.40)
Zone 2
a-value: 3.54(±0.45)
b-value: 0.82 (±0.12)
m max(obs): 8.1
m max: 8.80 (±0.20)
Zone 3
a-value: 1.96(±0.36)
b-value: 0.54 (±0.07)
m max(obs): 6.2
m max: 8.30 (±0.30)
Zone 4+5
a-value: 3.30(±0.08)
b-value: 0.75(±0.08)
m max(obs): 6.5
m max: 8.50 (±0.30)
Zone 6+7+11
a-value: 3.22(±0.59)
b-value: 0.84 (±0.16)
m max(obs): 6.8
m max: 7.20 (±0.30)
Zone 8+9
a-value: 4.25(±0.56)
b-value: 0.99 (±0.13)
m max(obs): 7.4
m max: 7.90 (±0.30)
Zone 10
a-value: 2.00 (±0.32)
b-value: 0.65 (±0.14)
m max(obs): 5.5
m max: 7.00 (±0.40)
Zone 12
a-value: 2.96(±0.63)
b-value: 0.77(±0.10)
m max(obs): 7.4
m max: 8.80 (±0.40)
Zone 13+14
a-value: 2.32(±0.63)
b-value: 0.63(±0.15)
m max(obs): 6.4
m max: 8.20 (±0.40)
Zone 15
a-value: 4.16(±0.41)
b-value: 0.99(±0.18)
m max(obs): 5.6
m max: 8.20 (±0.40)
Zone 16+17+26+31+32
a-value: 1.64(±0.45)
b-value: 0.57 (±0.15)
m max(obs): 5.8
m max: 6.80 (±0.30)
Zone 18
a-value: 5.93(±0.50)
b-value: 1.31 (±0.15)
m max(obs): 6.0
m max: 7.10 (±0.30)
Instrumental data
Incomplete data
GR
TGR
Slip rate
Log10 (λ)
Magnitude(MW)

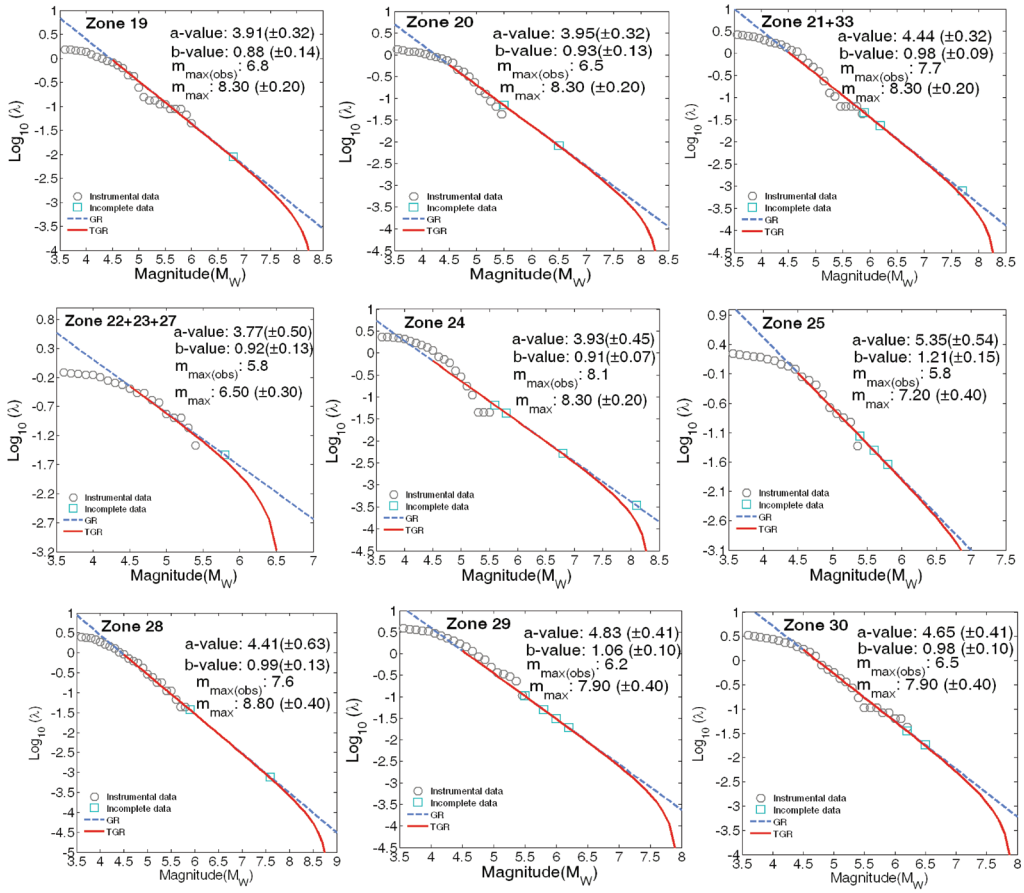

Figure 4.4 **Frequency magnitude distribution plots for mainshock events in each of the seismogenic source zones. The red line represents Truncated Gutenberg-Richter (TGR) relation, the blue line representing Gutenberg-Richter (GR) relation while the circles & squares represent the instrumental events (complete data coverage) and incomplete data (including the historical data as extreme data coverage) respectively.**

Table 4.2 **Estimated seismicity parameters for all the polygonal seismogenic sources considered for PSHA**

Zone	*b*-value	*a*-value	M_{max} (Predicted)	M_{max} (Observed)
Zone 1	0.73(±0.14)	3.02(±0.59)	7.70(±0.40)	6.9
Zone 2	0.82(±0.12)	3.54(±0.45)	8.80(±0.20)	8.1
Zone 3	0.54(±0.07)	1.96(±0.36)	8.30(±0.30)	6.2

Zone	*b*-value	*a*-value	M_{max} (Predicted)	M_{max} (Observed)
Zone 4+5	0.75(±0.08)	3.30(±0.08)	8.50(±0.30)	6.5
Zone 6+7+11	0.84(±0.16)	3.22(±0.59)	7.20(±0.30)	6.8
Zone 8+9	0.99(±0.13)	4.25(±0.56)	7.90(±0.30)	7.4
Zone 10	0.65(±0.14)	2.00(±0.32)	7.00(±0.40)	5.5
Zone 12	0.77(±0.10)	2.96(±0.63)	8.80(±0.40)	7.4
Zone 13+14	0.63(±0.15)	2.32(±0.63)	8.20(±0.40)	6.4
Zone 15	0.99(±0.18)	4.16(±0.41)	8.20(±0.40)	5.6
Zone 16+17+26+31+32	0.57(±0.15)	1.64(±0.45)	6.80(±0.30)	5.8
Zone 18	1.31(±0.15)	5.93(±0.50)	7.10(±0.30)	6.0
Zone 19	0.88(±0.14)	3.91(±0.32)	8.30(±0.20)	6.8
Zone 20	0. 93(±0.13)	3.95(±0.32)	8.30(±0.20)	6.5
Zone 21+33	0.98(±0.09)	4.44(±0.32)	8.30(±0.20)	7.7
Zone 22+23+27	0.92(±0.13)	3.77(±0.50)	6.50(±0.30)	6.2
Zone 24	0.91(±0.07)	3.93(±0.45)	8.30(±0.20)	8.1
Zone 25	1.21(±0.15)	5.35(±0.54)	7.20(±0.40)	5.8
Zone 28	0.99(±0.13)	4.41(±0.63)	8.80(±0.40)	7.6
Zone 29	1.06(±0.10)	4.83(±0.41)	7.90(±0.40)	6.2
Zone 30	0.98(±0.10)	4.65(±0.41)	7.90(±0.40)	6.5

4.2.4 Smoothed Seismicity Models

The contribution of background events in the hazard perspective is calculated using smoothened gridded seismicity models. It allows modeling of discrete earthquake distributions into spatially continuous probability distributions. The technique given by Frankel (1995) is employed here for seismicity smoothening. The technique have been previously employed by several workers (Frankel *et al.,* 2002; Stirling *et al.,* 2002; Lapajne *et al.,* 2003; Jaiswal and Sinha, 2007; Nath and Thingbaijam, 2012). In the present analysis, the study region is gridded at a regular interval of 0.1°; each grid point encompassing a cell of 0.1°×0.1°. The smoothened function is given as

$$N(m_r) = \frac{\sum_j n_j(m_r) e^{-\left(d_{ij}/c\right)^2}}{\sum_j e^{-\left(d_{ij}/c\right)^2}} \tag{4.4}$$

where, $n_j(m_r)$ is the number of events with magnitude $\geq m_r$, d_{ij} is the distance between i^{th} and j^{th} cells, and c denotes the correlation distance. The annual activity rate λ_{m_r} is computed each time as $N(m_r)/T$ where T is the sub-catalog period. The present analyses make use of sub-catalogs for

the periods 1990-2014, 1964-2014 and 1903-2014 with the threshold magnitudes of M_w 3.5, 4.5 and 5.5, respectively as summarized in Table 4.3 at the hypocentral depth ranges 0-25 km and 25-70 km as displayed in Figure 4.5. Correlation distances of 55 km, 65 km, and 85 km are decided for the respective cases by calibrating the outputs from several runs of the algorithm with the observed seismicity.

Table 4.3 **The sub-catalogs for the three different threshold magnitudes considered for the construction of seismicity grids**

Depth-range (km)	Sub-catalog (threshold magnitude)		
	M_w 3.5	M_w 4.5	M_w 5.5
0–25	1990–2014	1964–2014	1900–2014
25–70	1990–2014	1964–2014	1902–2014

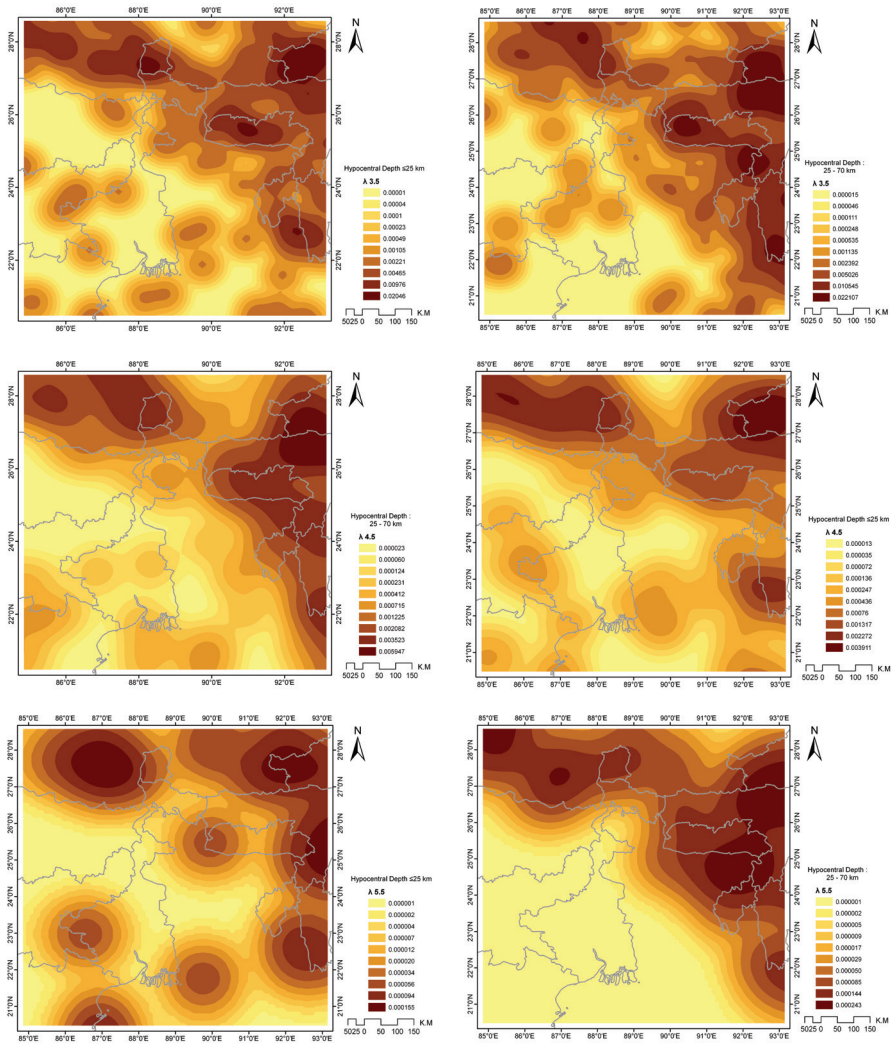

Figure 4.5 **Smoothened seismicity models in Bengal Basin for different threshold magnitudes at two hypocentral depth range.**

It is seen that at the threshold magnitude 3.5 patches of stress concentration in terms of clustered activity rate are seen within the Bengal Basin itself, while at higher threshold magnitudes, maximum stress accumulation is seen to occur in the northeast and northwestern part of West Bengal. At higher hypocentral depth range *i.e.* at 25-70 km the stress is seen to accumulate in the Arakan Yoma subduction belt as the activity rate concentration is high there.

4.2.5 Tectonic Seismicity Activity Rate Analysis

In the present study, seismicity activity rates are also calculated for each active tectonic source using three different threshold magnitudes of M_w 3.5, M_w 4.5 and M_w 5.5 depending upon different focal depth ranges <25 km and 25-70 km. The tectonic based seismic activity has been estimated by fault degradation technique following the methodology of Iyengar and Ghosh (2004). The number of earthquake occurrences per year with $m>m_o$ in a given source zone consisting of n number of faults is denoted as $N(m_o)$. According to the fault degradation technique $N(m_o)$ should be equal to the sum of the number of earthquakes $N_s(m_o)$ that is possible to occur at different faults available in the source zone *i.e.* $N(m_o)=\sum N_s(m_o)$, where $N_s(m_o)$ represents the annual frequency of occurrence of an event on s^{th} subfault (s=1,2….n) and m_o of 3.5, 4.5 and 5.5 have been used based on the threshold magnitudes. The number of events $N_s(m_o)$ that occurs on a given fault depends upon various factors like the fault length and past seismicity associated with the fault. Thus the two parameters length of the fault (L_s) and the number of past earthquakes (n_s) of magnitude m_o associated with the s^{th} fault have been used as weights for estimating $N_s(m_o)$. If N_t is the total number of events occurred within the source zone the weighting factor is estimated as

$$\alpha_s = L_s / \Sigma L_s \qquad and \qquad \delta_s = n_s / N_t \tag{4.5}$$

Taking the mean of the above two weight factors as indicating the seismic activity of the s^{th} fault in the zone we get

$$N_s(m_o) = 0.5(\alpha_s + \delta_s) * N(m_o) \tag{4.6}$$

The annual activity rate of each tectonic feature has been computed using the above expression where the regional recurrence is degraded into individual faults/lineaments. Figure 4.6 depicts the tectonic annual activity rate for different threshold magnitudes at both the aforementioned hypocentral depth ranges.

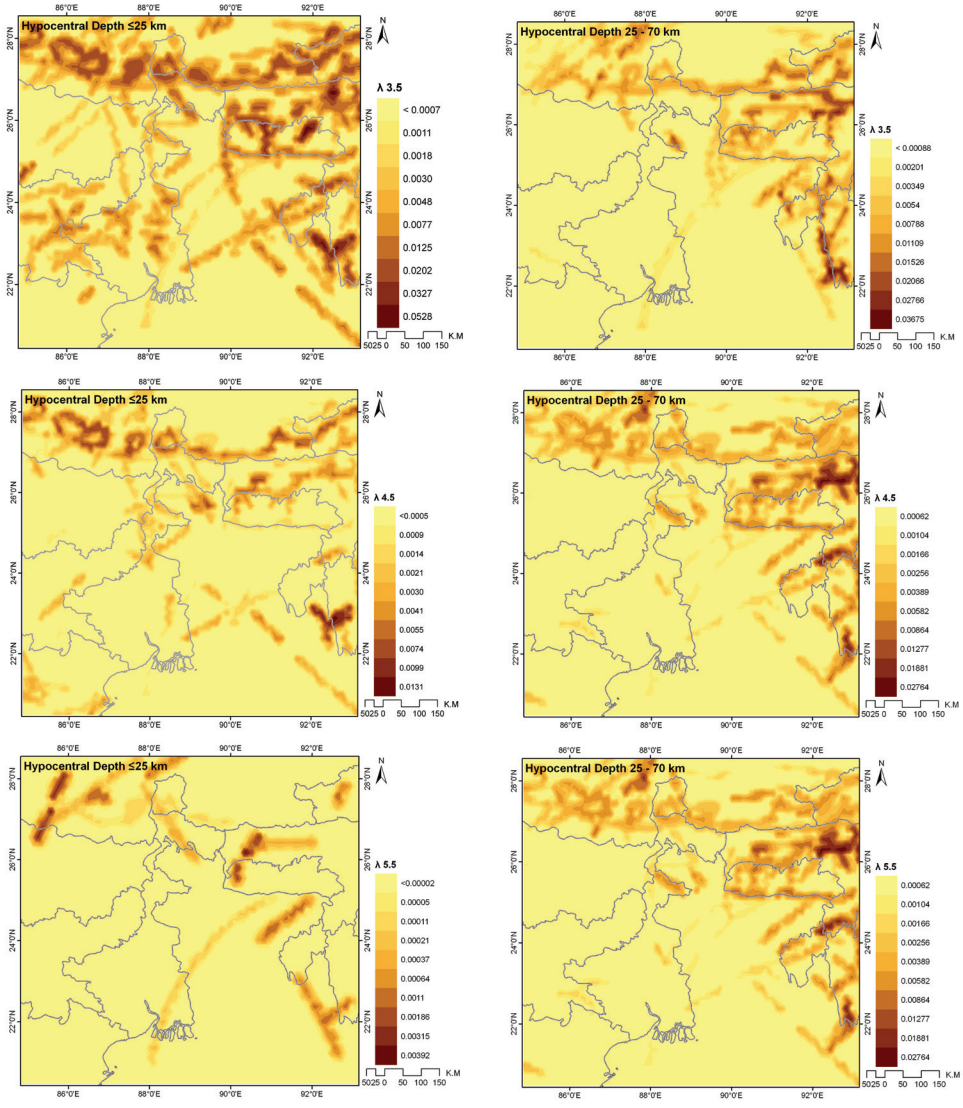

Figure 4.6 **Tectonic activity rates for different threshold magnitudes at two hypocentral depth ranges.**

4.2.6 Ground Motion Prediction Equations

The damages and ground failure due to an earthquake occur mainly because of the ground shaking. Seismic hazard analysis estimates these ground shaking parameter in terms of PGA, PGV and PSA for a region. Regional specific Ground Motion Prediction Equation (GMPE) is an important input to the seismic hazard model. The ground motion parameters at a site of interest

are evaluated by using a ground motion prediction equation that relates a specific strong motion parameter of ground shaking to one or more seismic attributes (Campbell and Bozorgnia, 2003). The appropriate ground motion prediction equations are not only useful in rapid hazard assessment but also important for seismic risk analysis. The selection of a model for the prediction equation is important since it should be realistic as well as a practical one, neither too complex nor too simple. In the study region a strong motion network recorded several moderate magnitude earthquakes (Nath, 2004; Pal *et al.,* 2008; Raj *et al*., 2008) from the near and distant fields from within the Bengal Basin, East Central Himalaya & Northeast India. Due to paucity of good magnitude coverage of strong ground motion data, analytical or numerical approaches for a realistic prognosis of possible seismic effects in terms of tectonic regime, earthquake size, local geology, and near fault conditions necessitate systematic ground motion synthesis. In order to strengthen the ground motion data base, the seismic events of small to moderate magnitude recorded by the Darjeeling-Sikkim Strong Motion Network (DSSMN) of IIT Kharagpur, PESMOS (http://pesmos.in) of IIT Roorke, IIT Guwahati strong motion network in the Northeast India region and the IIT Kharagpur Broadband Seismological Observatory have been amalgamated with the simulated ones. There are several algorithms available for ground motion synthesis. However, finite-fault stochastic method is considered to be best suited over a large fault rupture distance and the source characteristics for near field approximation.

The stochastic approach is one of the most expedient methods of synthesizing strong ground motion and is modeled with Gaussian noise using a spectrum that is either empirical or based on a physical model of the earthquake source (Halldorsson *et al.,* 2002). The stochastic algorithm uses standard convolution theorem to model spectral acceleration. The amplitude spectrum A(ω) can be written, in the frequency domain, as the product of source function SO(ω, ω_c), a propagation path term P(ω), and a site function SI(ω) (Boore 1983; Nath *et al.,* 2009) as given below

$$A(\omega) = SO(\omega, \omega_c).SI(\omega).P(\omega) \tag{4.7}$$

where $\omega_c = 2\pi f_c$ refers to corner frequency. The conventional point source approximation is unable to characterize key features of ground motions from large earthquakes, such as their long duration and the dependence of amplitudes and duration on the azimuth to the observation point (source directivity). A finite source model is, thus, used to simulate ground motion that contributes not only to the duration and directivity but also affects the shape of the spectra of seismic waves. The dynamic corner frequency approach (Motazedian and Atkinson, 2005) allows the dynamic evolution of the corner frequency of the fault rupture; as the rupture grows frequency content of the radiated seismic waves shifts to lower frequencies. In the stochastic finite-fault simulation technique, a large fault is divided into *N* number of sub-faults, and each sub-fault is considered as a point source. The ground motions from each sub-fault is calculated by the stochastic point-source method and are summed with a proper time delay in the time domain to obtain the ground motion from the entire fault, *A(t)*

$$A(t) = \sum_{i=1}^{nl} \sum_{j=1}^{nw} H_{ij} * A_{ij}(t - \Delta t_{ij}) \tag{4.8}$$

where *nl* and *nw* are the number of sub-faults along the length and width of the main fault, H_{ij} is a normalization factor for the ij^{th} sub-fault that aims to conserve energy and Δt is the relative time delay for the radiated wave. For each sub-fault, seismic moment M_{0ij}, corner frequency fc_{ij}, and normalization factor H_{ij} need to be specified. The moment of the n^{th} sub-fault is calculated using the slip distribution as follows

$$M_{0ij} = \frac{M_0 * s_{ij}}{\sum_{i=1}^{nl}\sum_{j=1}^{nw} s_{ij}} \tag{4.9}$$

where s_{ij} is the slip of the ij^{th} sub-fault and M_0 is the seismic moment. The dynamic corner frequency is expressed as

$$fc_{ij} = 4.9*10^6 N_R(t)^{-1/3} N^{1/3} \beta(\Delta\sigma / M_0)^{1/3} \tag{4.10}$$

where $N_R(t)$ is the number of rupture sub-faults at a time t, N refers to total number of sub-faults totaling to $N_R(t)$ at the end of the rupture and $\Delta\sigma$ is the stress drop. The normalization scaling factor responsible for conserving energy at the high frequency spectral level of the sub-faults is defined by

$$H_{ij} = (N\sum\{f^2/[1+(f/f_o)^2]\}/\sum\{f^2/[1+(f/f_{oij})^2]\})^{1/2} \tag{4.11}$$

where, f_0 is the corner frequency of the entire fault length. The high-frequency energy radiated from all the sub-faults is assumed to be equal, with the sum being constrained by the total high-frequency energy of the earthquake, as implied by its Fourier spectral acceleration amplitude at high frequencies. Thus in the present study the stochastic finite-fault simulation package EXSIM developed by Motazedian and Atkinson (2005) have been implemented for strong ground motion synthesis. In order to create a strong ground motion database we simulated earthquakes of M_w 3.5 to the Maximum Credible Earthquake magnitude in the three tectonic provinces namely the East Central Himalaya, Bengal Basin and Northeast India at 0.2 M_w intervals. The source functions for earthquake simulation using EXSIM package have been obtained from literature review as given in Table 4.4. The amplification due to the shallow crustal effects, considered an important attribution for ground motion simulation at the crustal level is used in the analysis and synthesis performed in this study. The crustal velocity structure of the Bengal Basin inferred by Mitra *et al.* (2008) as shown in Figure 4.7(a) has been used for the calculation of the crustal amplification. The crustal level amplification as a function of frequency is calculated from the shear-wave velocity profile using the quarter wavelength approximation (Boore and Joyner, 1997). The crustal model in our study (V_S^{30}~760 m/sec) is comparable with Atkinson and Boore (2006) for NEHRP B/C (soft) boundary site condition as depicted in Figure 4.7(b).

Table 4.4 **Parameters used for Strong Ground motion simulation (*)**

Parameter	East Central Himalaya source zone	Bengal Basin source zone	Northeast India source zone
Strike	285°	232°	112°
Dip	6°	32°	50°
Focal depth (km)	20	35.9	35
Source (Location)	27.55°N, 87.09°E	21.6°N, 88.07°E	26.0°N, 91.0°E
Stress (bar)	275	30	159
Crustal density (g/cm^3)	2.7	2.7	2.7
Shear-wave velocity, β (km/s)	3.8	3.8	3.8
Quality factor	$167f^{0.47}$	$400f^{0.48}$	$372f^{0.72}$
Kappa	0.02	0.02	0.02
Geometrical spreading	1/R (R<100 km) $1/R^{0.5}$ (R>100 km)		
Windowing function	Saragoni and Hart (1974)		
Damping	5%		

*Source parameters have been adopted from Nath *et al.* (2010)

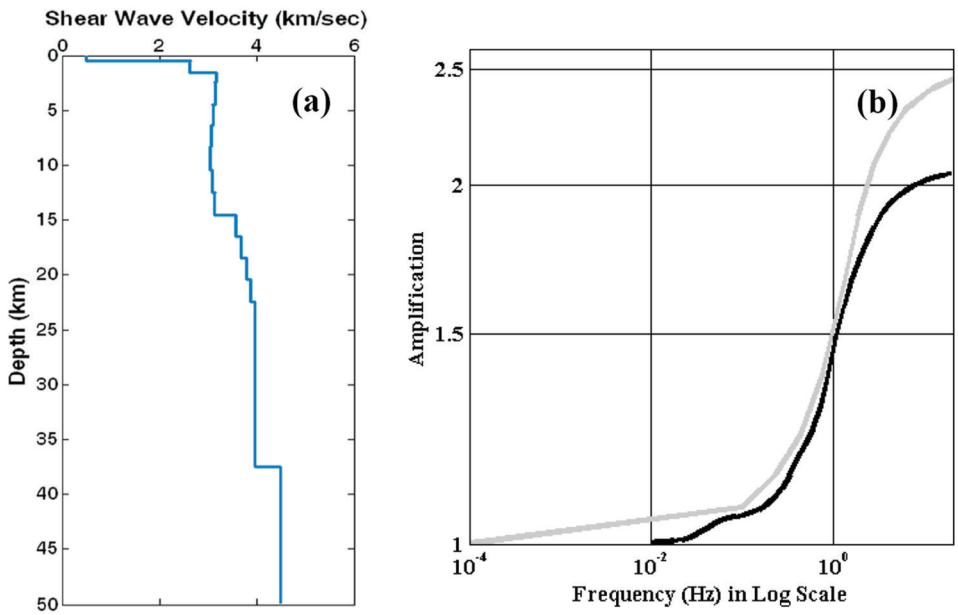

Figure 4.7 **(a) Crustal velocity model of the Bengal Basin (adopted from Kaila *et al.*, 1992 and Mitra *et al.*, 2008), and (b) Crustal amplification used in our study (dark line) as compared to that used by Atkinson and Boore (2006) for NEHRP B/C boundary sites (grey line).**

The simulated earthquakes have been validated with the recorded earthquake data from the Darjeeling-Sikkim Strong Motion Network (DSSMN) of IIT Kharagpur, PESMOS (http://pesmos.in) of IIT Roorke, IIT Guwahati strong motion network in Northeast India region and the IIT Kharagpur Broadband Seismological Observatory. Figure 4.8 exhibits a satisfactory agreement between the recorded and the simulated acceleration spectra of the 13th December 2005 earthquake of M_w 4.0 & 6th February 2008 earthquake of M_w 4.9 both recorded at the IIT Kharagpur Broadband Seismological Observatory for the Bengal Basin seismogenic source (Figures 4.8a-b); the 18th September 2011 Sikkim earthquake of M_w 6.9 recorded at Gangtok and Siliguri Strong Motion Stations of DSSMN for the East Central Himalaya seismogenic source (Figures 4.8c-d); the 18th August 2009 Myanmar-India Manipur Border earthquake of M_w 5.6 recorded at Guwahati, and the 4th February 2011 Myanmar-India Manipur Border earthquake of M_w 6.4 recorded at Jowai Strong Motion Station of PESMOS for Northeast India seismogenic source (Figures 4.8e-f).

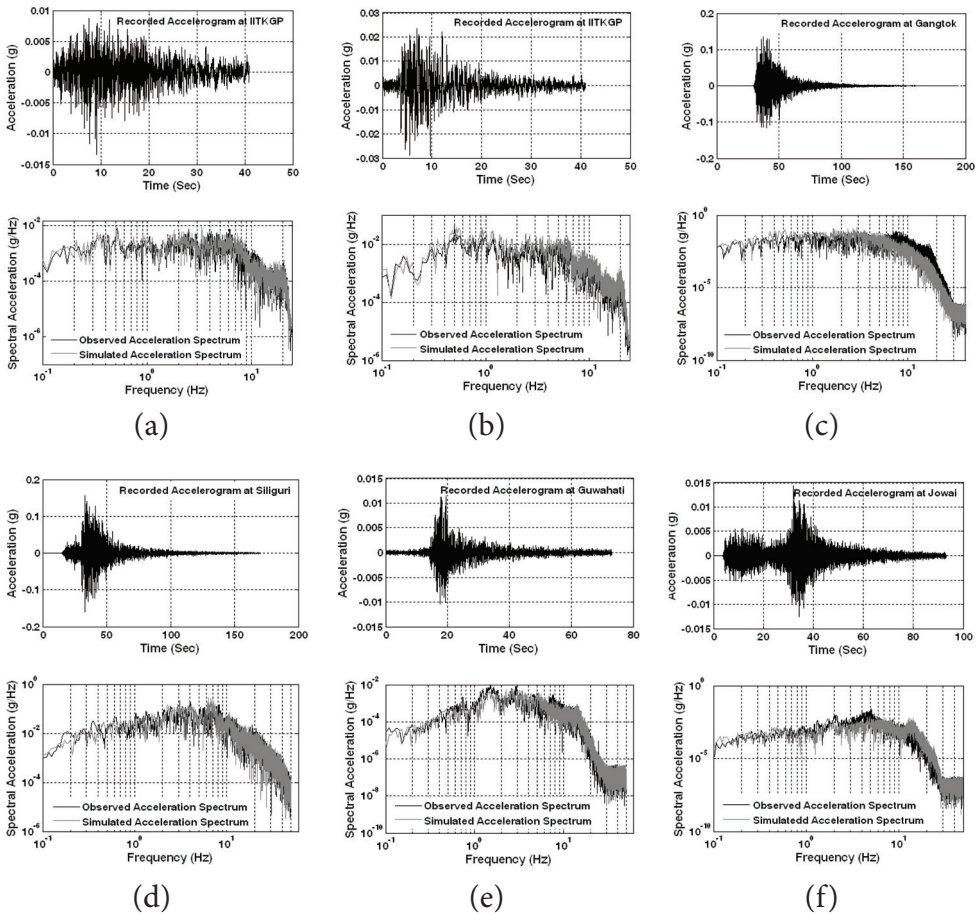

Figure 4.8 **Recorded accelerogram, and comparison of the observed & simulated acceleration spectra of: (a) 13th December 2005 earthquake of M_w 4.0 & (b) 6th February 2008 Earthquake of M_w 4.9 recorded at IIT Kharagpur (IITKGP) broadband observatory for Bengal Basin seismogenic source; (c) 18th September 2011 Sikkim Earthquake of M_w 6.9 recorded at Gangtok, & (d) Siliguri strong motion station of DSSMN for East Central Himalaya seismogenic source; (e) 18th August 2009 Myanmar-India Manipur Border Earthquake of M_w 5.6 recorded at Guwahati, & (f) 4th February 2011 Myanmar-India Manipur Border Earthquake of M_w 6.4 recorded at Jowai Strong Motion Station of PESMOS (http://pesmos.in) for Northeast India seismogenic source.**

Further a scatter plot shown in Figure 4.9 between the recorded and the synthesized PGA values for a wide magnitude range of M_w 3.9 to 6.9 considering all the three seismogenic sources *viz*. Bengal Basin, East Central Himalaya & Northeast India depicts a 1:1 correspondence establishing the efficacy of earthquake synthesis and its utility in conjunction with the recorded ones in the creation of a significant strong ground motion data base for working out the Next Generation Attenuation models in the present study for probabilistic seismic hazard assessment of the region. Thereupon nonlinear regression analyses were performed for different shaking parameters Y (*i.e.* PGA, PGV and PSA at different periods) following least square error minimization to estimate the coefficients of Next Generation Attenuation (NGA) models following Atkinson and Boore (2006) & Campbell and Bozorgnia (2003) as given in equation (4.12) and (4.13), respectively, for the three major tectonic provinces *viz*. East Central Himalaya, Bengal Basin, and Northeast India.

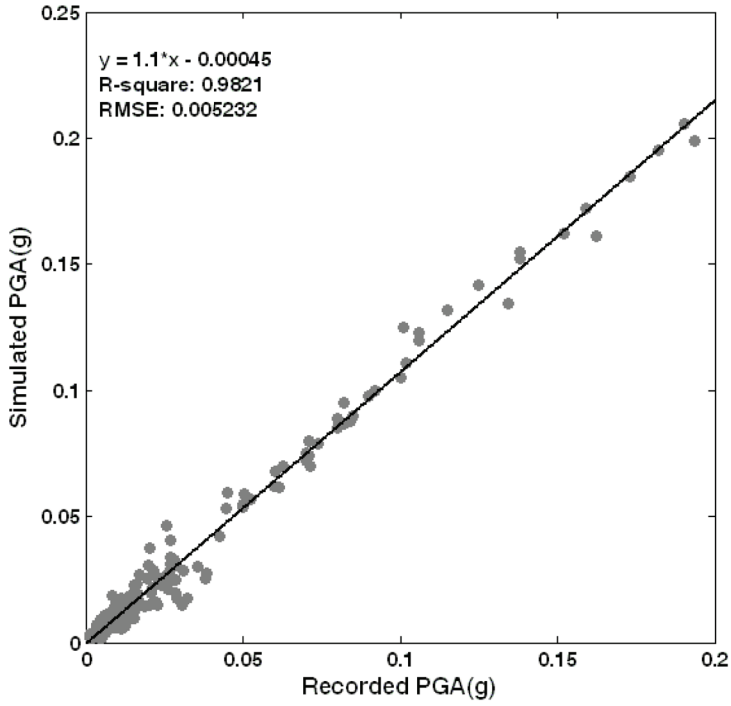

Figure 4.9 **Scatter plot between the recorded and the synthesized PGA values for a wide magnitude range of M_w 3.9 to 6.9 considered in all the three seismogenic sources *viz*. Bengal Basin, East Central Himalaya and Northeast India.**

The Fundamental models adopted for nonlinear regression analysis is given as

(a) Atkinson and Boore, 2006 (BA 06):

$$LogPSA = C_1 + C_2M + C_3M^2 + (C_4 + C_5M)f_1 + (C_6 + C_7M)f_2 + (C_8 + C_9M)f_0 + C_{10}R_{cd} \quad (4.12)$$

where

$$f_0 = \max(\log(R_0 / R_{cd}), 0); f_1 = \min(\log R_{cd}, \log R_1);$$
$$f_2 = \max(\log(R_{cd} / R_2), 0); R_0 = 10; R_1 = 70; R_2 = 140$$

M is the magnitude in M_w, R_{cd} represents fault distance in km and $C_1 \ldots C_{10}$ are the regression coefficients. The obtained regression coefficients for three dominant tectonic provinces using this Next Generation Attenuation model are given in Table 4.5.

Table 4.5 **Regression Coefficients considering Atkinson and Boore (2006) NGA model for three tectonic regimes**

East Central Himalaya Source											
PSA(sec)	C_1	C_2	C_3	C_4	C_5	C_6	C_7	C_8	C_9	C_{10}	Std(δ)
0.05	0.628	0.798	-0.049	-1.256	0.061	-1.767	0.254	0.539	-0.198	-0.0039	0.208
0.08	0.680	0.753	-0.043	-0.970	0.030	-1.535	0.301	0.514	-0.181	-0.0047	0.257
0.1	0.919	0.730	-0.044	-1.286	0.070	-2.480	0.315	0.337	-0.147	-0.0036	0.205
0.2	1.080	0.717	-0.049	-1.388	0.112	-2.153	0.351	0.806	-0.156	-0.0049	0.175
0.3	1.073	0.730	-0.050	-2.093	0.201	-1.070	0.218	-0.110	-0.040	-0.0042	0.160
0.5	0.114	0.954	-0.065	-2.159	0.209	-1.222	0.231	0.884	-0.185	-0.0039	0.159
1	-1.306	1.281	-0.089	-2.309	0.231	-0.785	0.199	0.826	-0.182	-0.0036	0.164
2	-4.666	2.061	-0.138	-2.343	0.220	-0.093	0.112	0.952	-0.207	-0.0035	0.157
5	-8.522	2.741	-0.166	-2.120	0.194	-0.080	0.099	0.979	-0.217	-0.0035	0.156
PGA	0.724	0.674	-0.044	-1.070	0.074	-1.510	0.281	2.052	-0.357	-0.0054	0.201
PGV	-0.669	0.840	-0.049	-1.898	0.129	-2.107	0.389	0.085	-0.112	-0.004	0.117
Bengal Basin Source											
PSA(sec)	C_1	C_2	C_3	C_4	C_5	C_6	C_7	C_8	C_9	C_{10}	Std(δ)
0.05	3.428	0.221	-0.033	-2.828	0.328	-0.936	0.231	-2.128	0.263	-0.0053	0.131
0.08	3.368	0.206	-0.030	-2.701	0.319	1.569	-0.040	-2.189	0.291	-0.0059	0.132
0.1	3.159	0.272	-0.029	-2.666	0.291	0.426	0.020	-2.002	0.232	-0.0051	0.128
0.2	3.081	0.296	-0.031	-2.725	0.308	1.260	-0.014	-2.076	0.213	-0.0057	0.142
0.3	2.705	0.304	-0.028	-2.449	0.274	1.107	0.022	-2.086	0.246	-0.0054	0.124
0.5	2.095	0.396	-0.032	-2.476	0.278	1.397	-0.026	-2.174	0.232	-0.0051	0.137
1	1.148	0.580	-0.045	-2.443	0.274	1.163	-0.022	-2.445	0.292	-0.0045	0.142
2	-1.622	0.942	-0.049	-2.205	0.235	1.107	-0.021	-2.224	0.271	-0.0041	0.143
5	-1.726	0.862	-0.047	-2.280	0.254	1.099	-0.025	-2.290	0.289	-0.0042	0.181
PGA	0.515	0.614	-0.042	-1.041	0.107	-1.090	0.204	2.977	-0.406	-0.0063	0.153
PGV	1.543	0.275	-0.027	-2.692	0.294	0.627	0.057	0.085	-0.069	-0.0048	0.171

Northeast India Source											
PSA(sec)	C_1	C_2	C_3	C_4	C_5	C_6	C_7	C_8	C_9	C_{10}	Std(δ)
0.05	0.770	0.650	-0.032	-1.077	0.060	0.592	0.141	0.090	-0.098	-0.0069	0.112
0.08	0.666	0.662	-0.032	-0.917	0.039	0.822	0.095	0.214	-0.121	-0.006	0.112
0.1	0.698	0.666	-0.031	-1.016	0.047	0.860	0.088	0.337	-0.147	-0.0059	0.108
0.2	0.789	0.676	-0.032	-1.028	0.046	0.494	0.086	0.606	-0.166	-0.0058	0.116
0.3	0.703	0.721	-0.039	-1.121	0.058	0.298	0.088	0.610	-0.159	-0.0054	0.109
0.5	0.470	0.730	-0.032	-1.283	0.054	0.654	0.045	0.388	-0.175	-0.0049	0.116
1	-0.325	0.751	-0.035	-1.163	0.080	0.483	0.068	0.826	-0.162	-0.0044	0.161
2	-0.609	0.581	-0.018	-0.966	0.061	0.463	0.071	0.952	-0.177	-0.0041	0.227
5	-0.683	0.521	-0.011	-1.055	0.051	0.710	-0.068	-0.179	-0.077	-0.0034	0.138
PGA	0.743	0.680	-0.040	-1.270	0.073	-1.460	0.226	0.446	-0.122	-0.0041	0.378
PGV	-0.423	0.731	-0.045	-1.749	0.146	0.202	0.223	0.085	-0.069	-0.0056	0.116

(b) Campbell and Bozorgnia, 2003 (CB 03):

$$\ln Y = c_1 + f_1(M_w) + c_4 \ln\sqrt{f_2(M_w, r_{seis}, S)} + f_3(F) + f_4(S) \tag{4.13}$$

where

$$f_1(M_w) = c_2 M_w + c_3(8.5 - M_w)^2,$$
$$f_2(M_w, r_{seis}, S) = r^2{}_{seis} + g(S)^2(\exp[c_8 M_w + c_9(8.5 - M_w)^2])^2,$$
$$g(S) = c_5 + c_6(S_{VFS} + S_{SR}) + c_7 S_{FR},$$
$$f_3(F) = c_{10} F_{RV} + c_{11} F_{TH},$$
$$f_4(S) = c_{12} S_{VFS} + c_{13} S_{SR} + c_{14} S_{FR}$$

S_{VFS}=1 (very Firm soil), S_{SR}=1 (Soft rock), S_{FR}=1 (Firm rock), S_{VFS}= S_{SR}=S_{FR}=0 (Firm soil), F_{TH}=1 (Thrust faulting), F_{RV}=1 (Reverse), F_{RV}=F_{TH}=0 (Strike-slip and Normal). M_w represents Moment magnitude and r_{seis} represents the closest distance to seismogenic rupture. According to Campbell and Bozorgnia (2003), the nonlinear site effects inherent in large ground motion on firm soil do not permit a significant increase in ground motion over the hanging wall effect. Moreover the hanging wall effect dies out for r_{seis}<8 km, or sooner if r_{jb} ≥5 km or δ ≥ 70º. Hence in the present scenario hanging wall effect is not considered and the prediction equation has been modified after Campbell and Bozorgnia (2003) to generate a New Generation Attenuation model suitable for the entire West Bengal region. The obtained regression coefficients for the three main tectonic provinces using this NGA model are given in Table 4.6.

Table 4.6 **Regression Coefficients considering Campbell and Bozorgnia (2003) NGA model for three tectonic regimes**

East Central Himalaya Source															
PSA(sec)	C_1	C_2	C_3	C_4	C_5	C_6	C_7	C_8	C_9	C_{10}	C_{11}	C_{12}	C_{13}	C_{14}	Std(δ)
0.05	-3.104	0.970	-0.034	-1.547	0.0106	-0.0039	0.052	0.809	0.084	0.479	0.436	-0.144	0.088	0.242	0.287
0.08	-3.046	0.865	0.064	-1.251	0.1221	-0.0051	-0.063	0.710	0.041	0.203	0.292	-0.151	0.143	-0.238	0.281
0.1	-3.133	0.882	0.063	-1.231	0.1449	-0.0051	-0.079	0.719	0.034	0.305	0.372	-0.142	0.196	-0.289	0.279
0.2	-2.902	0.861	0.066	-1.261	0.1395	-0.0045	-0.041	0.654	0.045	0.570	0.522	-0.146	0.247	-0.300	0.273
0.3	-2.614	0.952	0.064	-1.459	0.128	-0.0003	-0.025	0.751	0.040	0.290	0.334	-0.123	0.302	-0.238	0.372
0.5	-3.122	0.742	-0.109	-1.070	0.2801	-0.0003	-0.251	0.791	-0.140	0.474	0.518	-0.123	0.294	-0.070	0.537
1	-3.689	0.780	-0.110	-1.059	0.2716	0	-0.206	0.788	-0.176	0.326	0.335	-0.072	0.257	-0.239	0.492
2	-4.013	0.721	-0.142	-1.153	0.294	0	-0.226	0.729	-0.168	0.414	0.445	-0.121	0.246	-0.234	0.360
5	-4.847	0.757	-0.129	-1.243	0.2807	0	-0.214	0.726	-0.170	0.275	0.299	-0.151	0.149	-0.204	0.430
PGA	-3.777	1.101	0.037	-1.586	0.0108	-0.005	-0.096	0.759	0.108	0.544	0.536	-0.123	-0.082	-0.293	0.352
PGV	-0.781	1.134	0.030	-1.272	0.0361	-0.005	-0.017	0.822	0.149	0.343	0.351	-0.123	0.476	-0.625	0.374
Bengal Basin Source															
PSA(sec)	C_1	C_2	C_3	C_4	C_5	C_6	C_7	C_8	C_9	C_{10}	C_{11}	C_{12}	C_{13}	C_{14}	Std(δ)
0.05	-4.732	1.040	0.046	-1.212	0.0458	-0.005	-0.080	0.784	0.096	0.243	0.333	-0.150	-0.272	-0.284	0.244
0.08	-2.852	0.837	0.056	-1.271	0.1261	-0.005	-0.068	0.779	0.044	0.243	0.333	-0.150	-0.082	-0.294	0.335
0.1	-2.582	0.812	0.039	-1.258	0.1464	-0.009	-0.060	0.674	0.093	0.224	0.313	-0.146	-0.184	-0.289	0.329
0.2	-3.296	0.950	0.021	-1.276	0.103	-0.014	-0.036	0.746	0.059	0.296	0.342	-0.148	-0.288	-0.264	0.318
0.3	-4.377	0.987	0.004	-1.192	0.0208	-0.002	-0.004	0.888	0.068	0.406	0.479	-0.123	0.229	-0.142	0.390
0.5	-4.694	1.027	0.029	-1.164	0.0228	-0.007	-0.046	0.874	0.100	0.216	0.279	-0.173	-0.108	-0.279	0.336
1	-3.440	0.762	-0.036	-1.175	0.0298	0	-0.065	0.786	0.097	0.329	0.338	-0.073	-0.149	-0.235	0.306
2	-4.737	0.757	-0.094	-0.939	0.0182	0	-0.041	0.854	0.012	0.060	0.064	-0.124	-0.212	-0.212	0.277
5	-5.777	0.733	-0.142	-0.857	0.0124	0	-0.019	0.876	0.126	0.061	0.057	-0.054	-0.597	-0.225	0.225
PGA	-4.734	1.027	0.031	-1.294	0.0228	-0.002	-0.092	0.744	0.110	0.406	0.479	-0.123	-0.108	-0.279	0.356
PGV	-0.540	1.086	0.023	-1.209	0.0408	-0.005	-0.015	0.828	0.144	0.343	0.351	-0.123	-0.645	-0.796	0.373
Northeast India Source															
PSA(sec)	C_1	C_2	C_3	C_4	C_5	C_6	C_7	C_8	C_9	C_{10}	C_{11}	C_{12}	C_{13}	C_{14}	Std(δ)
0.05	-2.184	0.767	0.036	-1.347	0.0896	-0.004	-0.049	0.789	0.088	0.274	0.334	-0.140	0.678	-0.231	0.269
0.08	-2.276	0.800	0.065	-1.348	0.114	-0.005	-0.067	0.790	0.057	0.302	0.392	-0.150	0.234	-0.222	0.269
0.1	-2.403	0.825	0.062	-1.295	0.1239	-0.009	-0.059	0.709	0.068	0.201	0.290	-0.146	0.485	-0.250	0.264
0.2	-2.152	0.840	0.034	-1.346	0.0925	-0.014	-0.041	0.743	0.085	0.374	0.320	-0.148	0.456	-0.280	0.256
0.3	-2.398	0.899	0.030	-1.470	0.0906	-0.002	-0.047	0.821	0.061	0.482	0.455	-0.123	0.458	-0.213	0.346
0.5	-2.182	0.798	-0.036	-1.324	0.0806	-0.002	-0.047	0.791	0.081	0.226	0.327	-0.123	0.494	-0.257	0.445
1	-3.260	0.810	-0.052	-1.211	0.084	0	-0.046	0.801	0.095	0.243	0.252	-0.073	0.335	-0.251	0.456
2	-4.129	0.585	-0.096	-0.903	0.0788	0	-0.047	0.750	0.086	0.403	0.407	-0.124	0.556	-0.244	0.336
5	-4.797	0.578	-0.099	-0.954	0.06107	0	-0.092	0.766	0.068	0.290	0.286	-0.054	0.153	-0.215	0.336
PGA	-3.230	0.870	0.040	-1.311	0.0609	0	-0.096	0.781	0.095	0.143	0.152	-0.073	0.335	-0.251	0.353
PGV	-1.455	1.071	0.052	-1.072	0.037	-0.005	-0.047	0.863	0.091	0.243	0.251	-0.123	0.231	-0.241	0.357

For establishing further efficacy of the analyses performed in the present study we generated a comparative plot of the predicted, recorded and simulated PGA values for the three aforesaid dominant seismogenic sources as shown in Figure 4.10 that exhibits a satisfactory agreement amongst all the three.

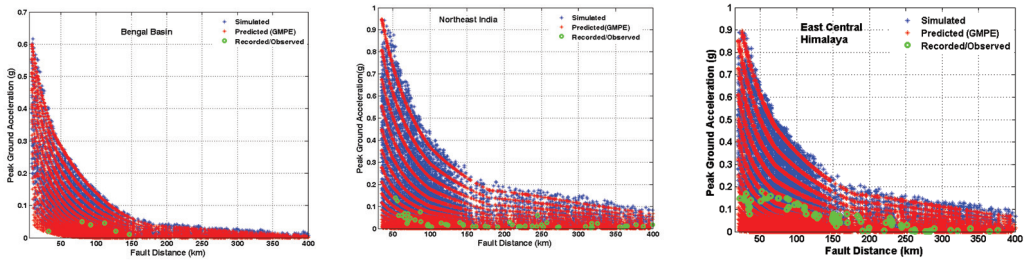

Figure 4.10 **The blue dots represent the simulated PGA the red dots represent the estimated PGA from Prediction equation, and the green dots represent the recorded PGA for three dominant seismic sources.**

The regression models for PGA and PSA have been validated using an analysis of residuals as

$$residual = \log_{10}\left(\frac{Y_{os}}{Y_p}\right) \tag{4.14}$$

where, Y_{os} is the recorded and simulated PGA/PSA, Y_p is the estimated PGA/PSA from the empirical attenuation relation. Residual plots for PGA as a function of fault distance for the three seismogenic sources are shown in Figure 4.11. It is evident that the residuals have a zero mean and are uncorrelated with respect to fault distance. A residual analysis of PGA and PSA of the NGA models predicted in the present investigation are unbiased with respect to both the magnitude & fault distance and hence can be used along with other existing prediction equations available for the region and also those available for similar tectonic setup in a logic tree framework for seismic hazard assessment.

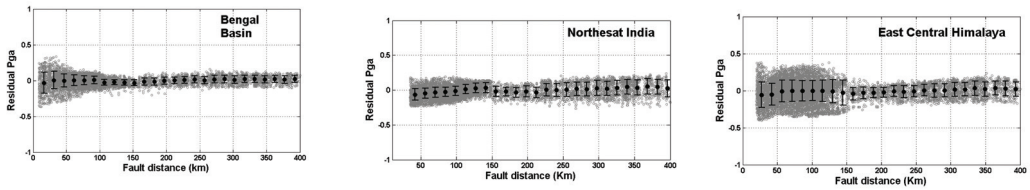

Figure 4.11 **Residuals of PGA with respect to fault distance for Bengal Basin, Northeast India and East Central Himalaya seismogenic sources.**

Apart from our own Prediction equations discussed above we have also incorporated some regional and global prediction relations based on the suitability testing for the estimation of seismic hazard of the region. Altogether we adopted a total of 14 Ground Motion Prediction Equations (GMPEs) as given in Table 4.7 for hazard computations in the region, whereas, the coefficients for the additional 8 GMPEs have been used as reported in the original publications. Appropriate selection and ranking of Ground Motion Prediction Equations (GMPEs) is critical for a successful logic-tree implementation in the probabilistic seismic hazard analysis. Quantitative suitability assessment, referred to as 'efficacy test', of a GMPE for a particular region is decisive in providing a ranking order for a suite of GMPEs towards the best possible selection. These are performed based on the efficacy test of the GMPEs towards suitability of adaptation in comparison with the observed earthquakes in the region. Towards this, we employed the information-theoretic approach proposed by Scherbaum *et al.* (2009). The efficacy test makes use of average sample log-likelihood (LLH) computation for the purpose of ranking. The method has been tested successfully by Delavaud *et al.* (2009) and applied to India by Nath and Thingbaijam (2011a). The probability consideration of LLH method is represented as

$$LLH = -\frac{1}{N}\sum_{i=1}^{N}\log_2(g(x_i)) \tag{4.15}$$

where, x_i represents the observed data for i = 1,...N. The parameter N is the total number of events.

Table 4.7 **Selected Ground Motion Prediction Equations for PSHA**

Selected Ground Motion Prediction Equations (GMPEs)	
Tectonic province	Reference and code in brackets
East Central Himalaya	Campbell and Bozorgnia, 2003 (CB 03); Atkinson and Boore, 2006 (BA 06); Sharma *et al.* 2009 (SHAR 09); Toro, 2002 (TORO 02); Campbell and Bozorgnia, 2008 (CAB 08)
Bengal Basin	Campbell and Bozorgnia, 2003 (CB 03); Atkinson and Boore, 2006 (BA 06); Raghukanth and Iyengar, 2007 (RI 07); Toro, 2002. (TORO 02)
Northeast India	Campbell and Bozorgnia, 2003 (CB 03); Atkinson and Boore, 2006 (BA 06); Nath *et al.* 2012 (NATH 12) (Shallow & Deep crust); Youngs *et al.* 1997 (YOUNGS 97); Campbell and Bozorgnia, 2008 (CAB 08)

The smaller the value of LLH, the higher is the ranking index of the GMPE. The ranking analyses were carried out using macroseismic intensity data (Martin and Szeliga, 2010) and the PGA– European Macroseismic Scale (EMS, Grünthal, 1998) relation at rock sites as given in Nath and Thingbaijam (2011a). Figure 4.12 represents the intensity as a function of distance for the indicated earthquakes derived from the ground motion prediction equations. The individual normalized weights of each GMPE have been derived by preparing a pair-wise comparison matrix (Saaty, 1980; 2000). The ranking analysis have been performed based on LLH values alongwith the weight assigned to each GMPE for three tectonic provinces as illustrated in Table 4.8. A sample pair-wise comparison matrix for the GMPEs used in Northeast India source zone and their normalized weights has been given in Table 4.9.

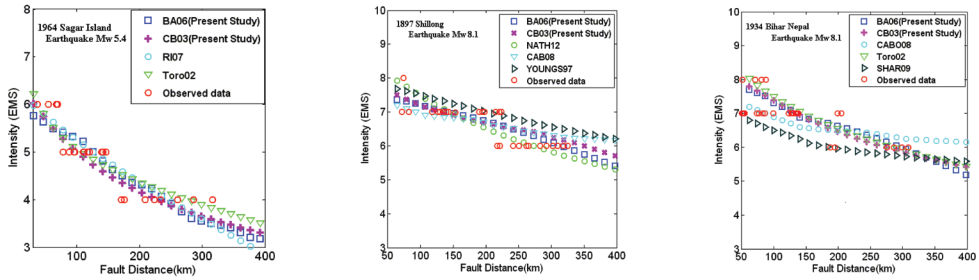

Figure 4.12 The intensity as a function of distance for the indicated earthquakes derived from the ground motion prediction equations for suitability testing of GMPEs.

Table 4.8 The weights and ranks assigned to respective GMPEs based on the average log likelihood (LLH) ranking in the three tectonic provinces

Bengal Basin			
Model	LLH	Rank	Weight
CB 03(Present Study)	2.169	1	0.4
BA 06 (Present Study)	2.189	2	0.3
RI 07	2.368	3	0.2
TORO 02	2.397	4	0.1
Northeast India			
Model	LLH	Rank	Weight
CB 03(Present Study)	2.306	1	0.33
BA 06 (Present Study)	2.331	2	0.27
NATH 12	2.370	3	0.20
CAB 08	2.545	4	0.13
YOUNGS 97	2.670	5	0.07
East Central Himalaya			
Model	LLH	Rank	Weight
CB 03(Present Study)	2.264	1	0.33
BA 06 (Present Study)	2.296	2	0.27
TORO 02	2.371	3	0.20
SHAR 09	2.412	4	0.13
CAB 08	2.712	5	0.07

Table 4.9 Pair-wise comparison matrix and normalized weights assigned to the GMPEs

Model	CB 03	BA 06	NATH 12	CAB 08	YOUNGS 97	Weight
CB 03	1	5/4	5/3	5/2	5/1	0.33
BA 06	4/5	1	4/3	4/2	4/1	0.27
NATH 12	3/5	3/4	1	3/2	3/1	0.20
CAB 08	2/5	2/4	2/3	1	2/1	0.13
YOUNGS 97	1/5	1/4	1/3	1/2	1	0.07

4.3 PSHA Computational Model

The seismic hazard at a particular site is usually quantified in terms of level of ground shaking observed in the region. The methodology for Probabilistic seismic hazard analysis incorporates how often the annual rate of ground motion exceeds a specific value for different return periods of the hazard at a particular site of interest. In the hazard computation all the relevant sources and possible earthquake events are considered. A synoptic probabilistic seismic hazard model of West Bengal and Kolkata is generated at Engineering Bedrock (V_s^{30}~760 m/s). The basic methodology of probabilistic seismic hazard analysis involves computation of ground motion thresholds that are exceeded with a mean return period of say 475 years/2475 years at a particular site of interest. The effects of all the earthquakes of different sizes occurring at various locations for all the seismogenic sources at various probabilities of occurrences are integrated into one curve that shows the probability of exceeding different levels of a ground motion parameter at the site during a specified time period. The computational formulation as developed by Cornell (1968), Esteva (1970) and McGuire (1976) is given as

$$\nu(a > A) = \sum_i \lambda_i \int_m \int_r \int_\delta P(a > A \mid m, r, \delta) f_m(m) f_r(r) f_\Delta(\delta) dm dr d\delta \qquad (4.16)$$

where ν ($a>A$) is the annual frequency of exceedance of ground motion amplitude A, λ, is the annual activity rate for the i^{th} seismogenic source for a threshold magnitude, function P yields probability of the ground motion parameter a exceeding A for a given magnitude m at source-to-site distance r. The corresponding probability density functions are represented by $f_m(m)$, $f_r(r)$ and $f_\Delta(\delta)$. The probability density function for the magnitudes is generally derived from the GR relation (Gutenberg and Richter, 1944). In practice this relationship is truncated at some lower and upper magnitude values which are defined as the truncation parameters related to the minimum (m_{min}) and maximum (M_{max}) values of magnitude, obtained by different methods. The present implementation makes use of the density function given by Bender (1983) as

$$f_m(m) = \frac{\beta \exp[-\beta(m - m_{\min})]}{1 - \exp[-\beta(M_{\max} - m_{\min})]} \tag{4.17}$$

where, $\beta = b \ln(10)$, and b refers to the *b-value* of GR relation. The distribution is bounded within a minimum magnitude $m_{\min}$ and a maximum magnitude $M_{\max}$. $f_\Delta(\delta)$ is the probability density function (in log-normal distribution) associated with the standard deviation of the residuals in GMPE. $f_\Delta(\delta)$ also defines the epsilon (ε) standard deviations of the ground motion from its median value through the prediction equation. The GMPEs are described as relationships between a ground motion parameter 'Y' (*i.e*. PGA, PGV or PSA at different periods), earthquake magnitude 'M', source-to-site distance 'R', and uncertainty or residual (δ) as

$$\ln(Y) = f(M, R) + \delta \tag{4.18}$$

The ground motion uncertainty δ is modeled as a normal distribution with a standard deviation, $\sigma_{\ln,y}$. Hence the above equation can be expressed as

$$\ln(Y) = f(M, R) + \varepsilon\sigma_{\ln,y} \tag{4.19}$$

where ε is the normalized residual, which is also a normal distribution with a constant standard deviation $\sigma_{\ln,y}$ is the standard deviation associated with the GMPE. In the PSHA formulation as given in equation (4.18) standard deviation denoted by δ is basically the residual associated with each GMPE. The probability density function $f_\Delta(\delta)$ follows a log normal distribution that can be expressed as

$$f_\Delta(\delta) = \frac{1}{\sqrt{2\pi}\sigma_{\ln,y}} \exp[-\frac{(\ln y - \ln y_{mr})^2}{2\sigma^2_{\ln,y}}] \tag{4.20}$$

where, $\ln y_{mr} = f(M,R)$ is the functional form of the prediction model in terms of magnitude, distance. Ground motion variability constitutes aleatory uncertainty intrinsic to the definition of GMPEs and consequently to that of PSHA. Computations based only on the median ground motions ignoring the associated variability are known to underestimate the hazards, especially at low annual frequencies of exceedance (Bommer and Abrahamson, 2006). The value of $\varepsilon_{\max}$ ranging from 2 to 4 has often been employed in probabilistic seismic hazard estimations (*e.g.* Marin *et al*., 2004). However, truncation at $\varepsilon_{\max}<3$ has been suggested to be inappropriate (*e.g*. Bommer and Abrahamson, 2006). In the present study, truncation at $\varepsilon_{\max}=4$ is considered to be pragmatic and implemented uniformly for all the GMPEs.

The distance probability function $f_r(r)$ represents the probability of occurrence of a given earthquake at a distance in the range (r, r+dr). In the present analysis instead of considering probability function for the source-to-site distance distinctively, we have implemented gridded-point locations within the source zone, where finite-fault ruptures are constructed based on the rupture dimensions estimated for each magnitude.

The hazard computation is performed using a Poisson occurrence model given by equation (4.21) below on grid-points covering the entire study region at a spacing of 0.005°.

$$P = 1 - e^{-\lambda t} \tag{4.21}$$

where λ is the rate of occurrence of the event (annual activity rate) and t is the time period of exceedance. With this, the annual rate of exceedance for an event with 10% probability in 50 years is given by

$$\lambda = -[\ln(1-0.1)/50] = 0.0021/yr \tag{4.22}$$

A Logic tree framework depicted in Figure 4.13 is employed in the computation at each site to incorporate multiple models in the source considerations, GMPEs and seismicity parameters. In the present study, the seismogenic sources *i.e.* tectonic & layered polygonal sources are assigned weights equal to 0.6 and 0.4, respectively. The three derivatives for the threshold magnitude of M_w 3.5, 4.5 and 5.5 are assigned weights equal to 0.20, 0.35 and 0.45, respectively. The seismicity model parameters, namely the annual rate of earthquakes $\lambda(m)$ and β pair are assigned weights of 0.36 while the respective ±1 standard deviation gets weight equal to 0.32. Similar weight allotment is assigned for M_{max}. The weights are allocated following the statistical rationale suggested by Grünthal and Wahlström (2006). In order to define appropriate weights, the percentage of probability mass in a normal distribution for the mean value and ±1 standard deviation are considered corresponding to the center of two equal halves.

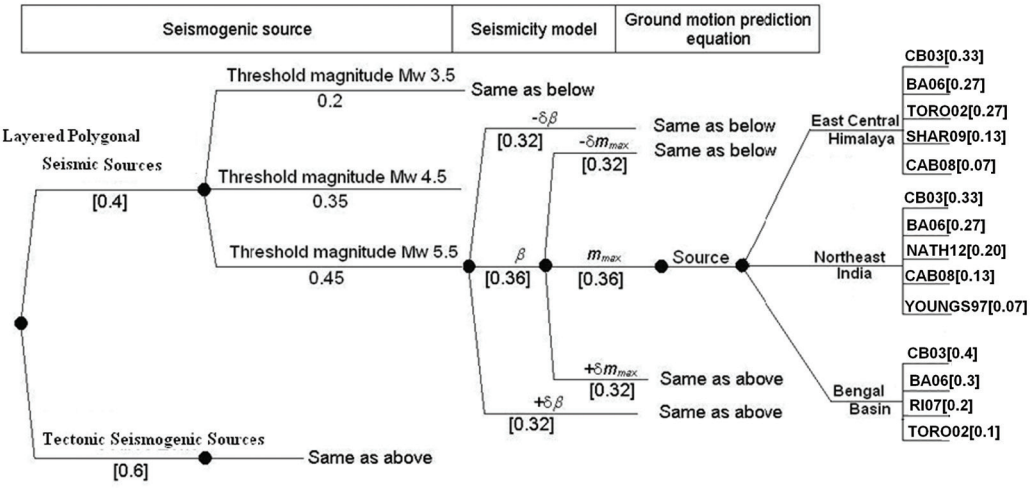

Figure 4.13 **A logic tree formulation for Probabilistic Seismic Hazard computation at each node of the region gridded at 0.005°× 0.005° intervals.**

4.4 Probabilistic Seismic Hazard Assessment of West Bengal at Engineering Bedrock

The hazard distributions are estimated for the source zones at both the depth ranges of 0-25 km and 25-70 km separately and integrated thereafter. Hazard curves show the probability of exceeding of different ground motion parameter at a particular site of interest. The hazard curves are important to compare hazards at different sites. The hazard curves are also useful in estimating expected losses at a particular site. Figure 4.14 depicts seismic hazard curves for selected cities of West Bengal *viz.* Haldia, Durgapur, Kolkata, Darjeeling, Kharagpur, Raiganj, Malda, Purulia, Bankura, Jalpaiguri, Bardhaman and Siliguri, corresponding to PGA, PSA at 0.2 sec and 1 sec respectively at engineering bedrock level. Both the 2% and 10% Probability of exceedance in 50 years have been demarcated by dotted lines in the diagram.

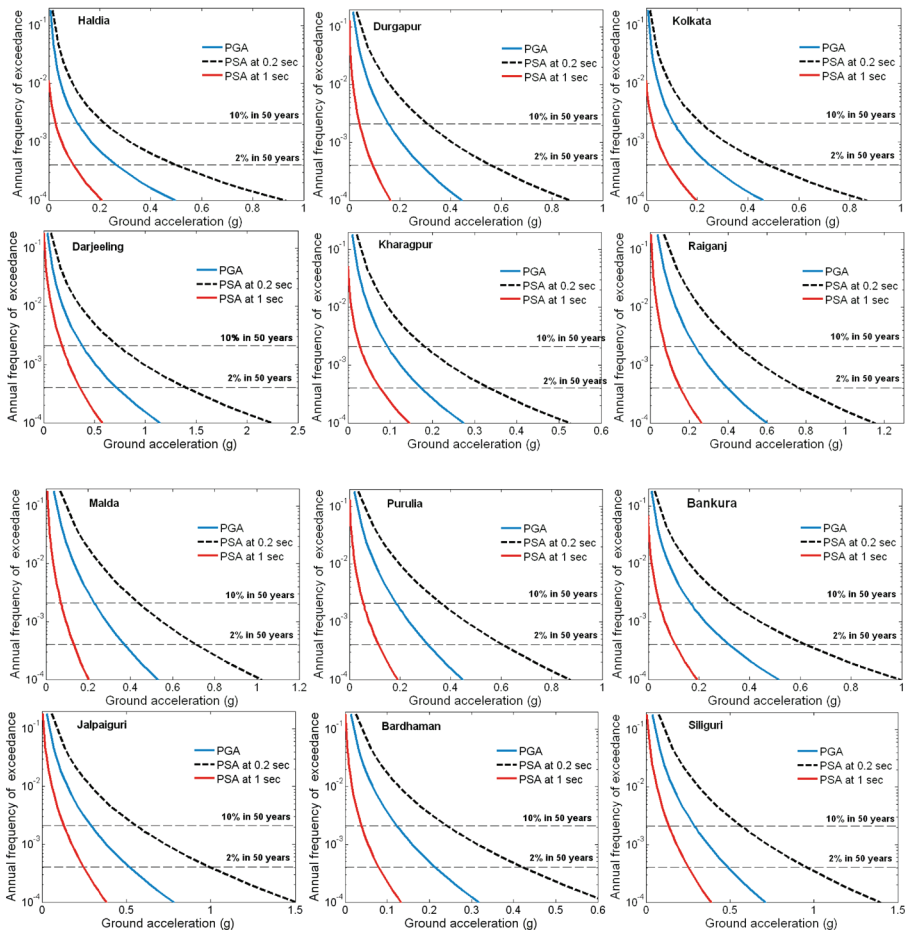

Figure 4.14 **The computed seismic hazard curves for selected cities of West Bengal corresponding to PGA, PSA at 0.2 sec and 1.0 sec respectively at engineering bedrock level.**

The spatial distribution of PGA at 10% probability of exceedance in 50 years owing to the contribution from the sources in both the hypocentral depth zones across Darjeeling and Cooch Behar region bounded by 87.75º E-90.1º E longitude and 25.9º N-27.3º N latitude situated in the Northern fringe of West Bengal is depicted in Figure 4.15. The hazard contributions for both the Layered Polygonal sources and Tectonic sources have been shown. It is observed that higher hazard contribution is attributed to the sources situated in the upper crust (0-25 km) region for both the Polygonal sources and the Tectonic ones with later contributing more than the aerial sources. In the case of lower crust (25-70 km), higher hazard has been observed in Darjeeling region with tectonic sources contributing more significantly than the polygonal ones. Following the same methodology the overall probabilistic seismic hazard distribution of West Bengal have been generated.

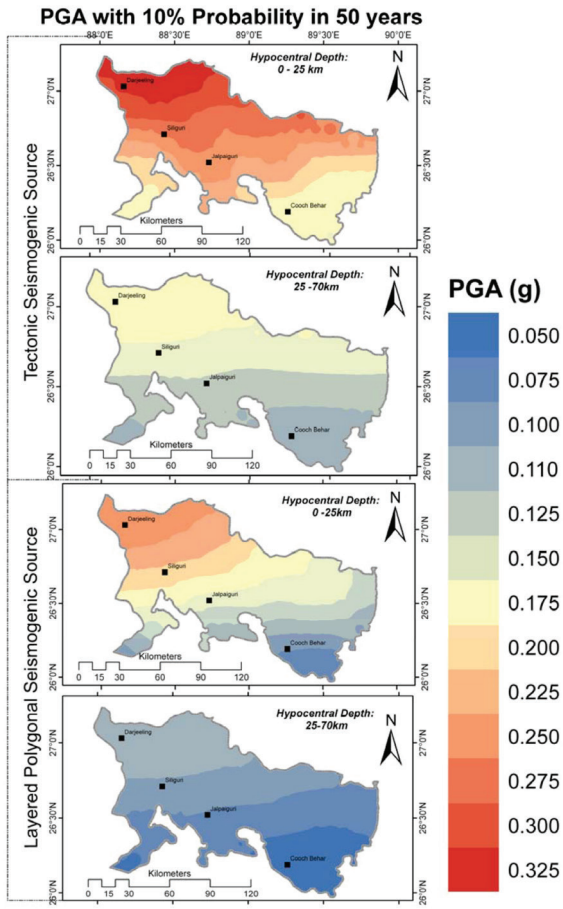

Figure 4.15 **The spatial distribution of PGA at each hypocentral depth range based on Tectonic and Layered Polygonal source bounded by 87.75° E to 90.1° E and 25.9° N to 27.3° N.**

The seismic hazard maps corresponding to the spatial distribution of PGA and PSA at 0.2 sec and 1.0 sec respectively for 10% probability of exceedance in 50 years with a return period of 475 years and 2% probability of exceedance in 50 years with a return period of 2475 years are shown in Figure 4.16. The PGA distribution across the region for 2% probability of exceedance in 50 years varies from 0.17g to 0.83g. The estimated maximum PGA of 0.83g is associated with Darjeeling and northern part of West Bengal region. Furthermore it has been observed that the regions in and around Raiganj, Malda, Purulia and Bankura exhibits relatively higher hazard. The 2% probability of exceedance in 50 years is generally considered to replicate deterministic seismic scenario of the region. The PSA distribution for short period at 0.2 sec varies from 0.33g to 1.60g while for longer period spectral acceleration at 1.0 sec varies from 0.07g to 0.39g.

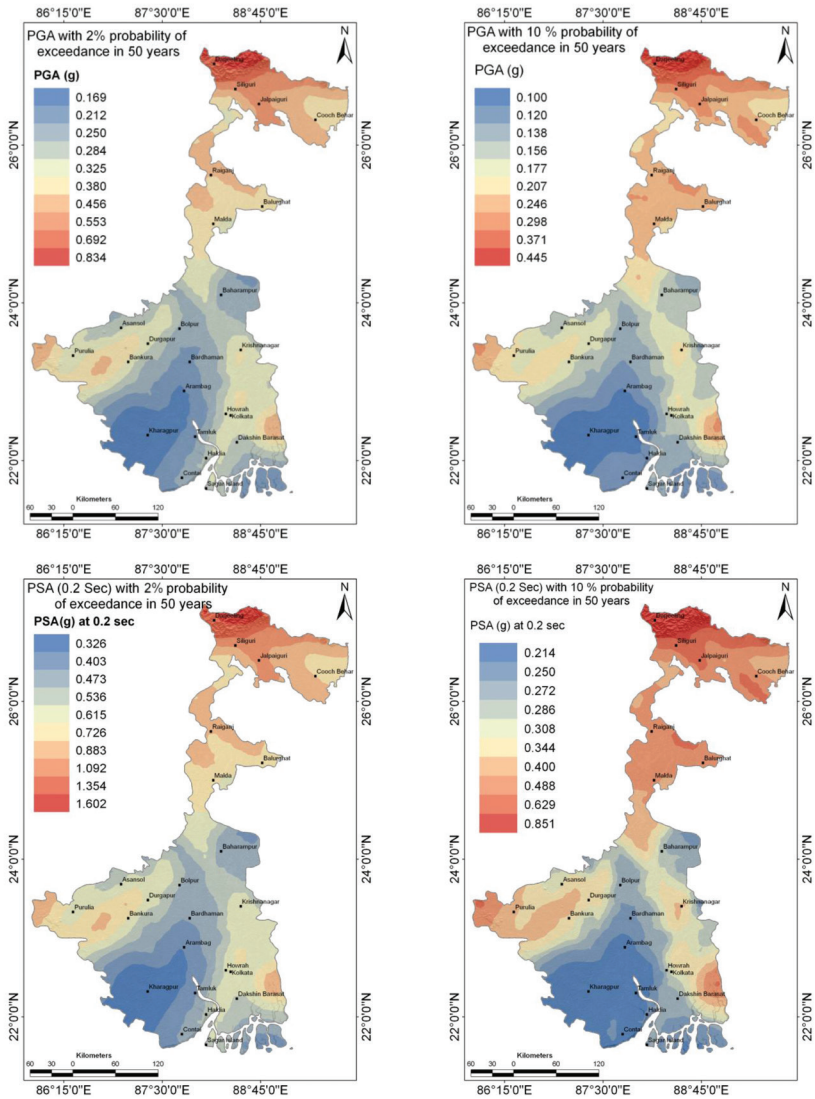

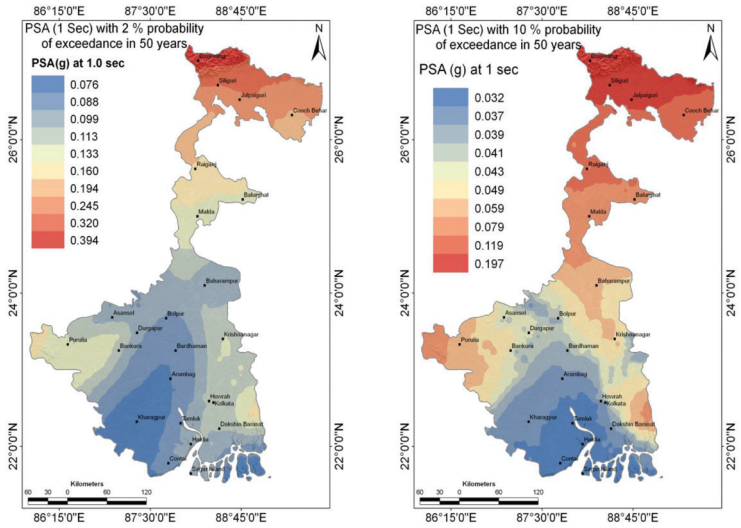

Figure 4.16 **Seismic hazard distributions in West Bengal in terms of PGA, PSA at 0.2 sec and 1.0 sec for firm rock site conditions.**

For the design purpose 10% probability of exceedance in 50 years are considered to be more appropriate and are practically used for the purpose of urbanization. The PGA distribution for 10% probability of exceedance in 50 years shows a variation from 0.10g to 0.44g for the entire West Bengal region. The State capital Kolkata shows a hazard level to the tune of 0.145g. The PSA at 0.2 sec exhibits a variation from 0.21g to 0.85g while for 1.0 sec it ranges from 0.03g to 0.19g. The associated statistical error in terms of ±standard deviation distribution for the assessment of probabilistic seismic hazard in West Bengal is depicted in Figure 4.17.

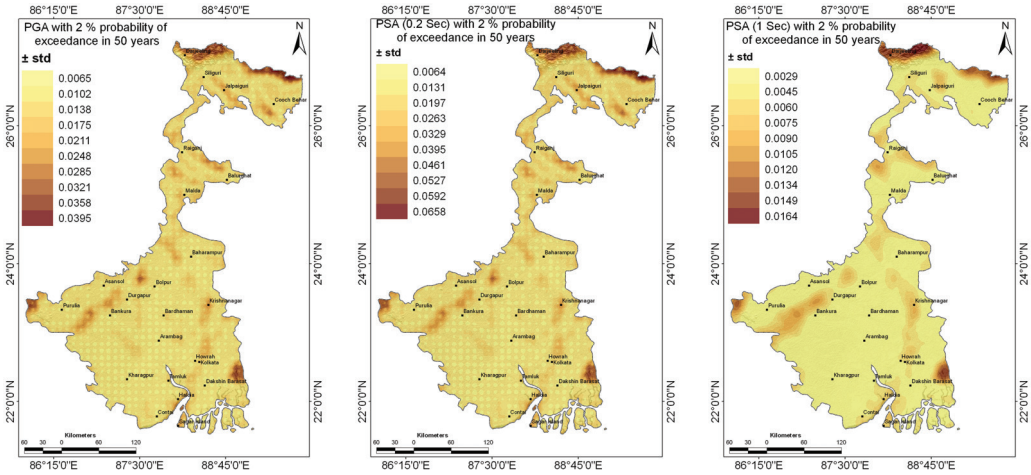

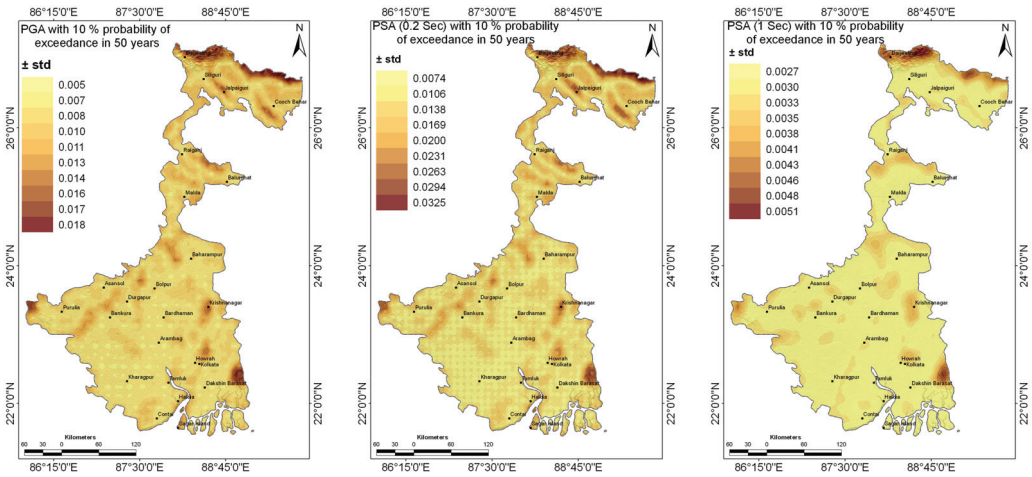

Figure 4.17 **The standard deviation (±σ) associated with PSHA of West Bengal at both 2% and 10% probability of exceedance in 50 years.**

The seismic hazard model presented here represents significant improvements over the deterministic zonation of BIS (2002) as well as the probabilistic map presented earlier by the other researchers. Table 4.10 illustrates and compares the computed PGA for 10% probability of exceedance in 50 years at firm rock site presented in this study with those estimated by GSHAP (Giardini *et al.,* 1999), Nath and Thingbaijam (2012) and earlier studies at selected locations of West Bengal.

Table 4.10 **Comparison of rock level PGA estimated in this study for 10% probability of exceedance in 50 years values with those provided by earlier studies**

Locations	Rock level PGA (g) with 10% Probability of exceedance in 50 years			
	Present Study	Previous Studies		
Kolkata	0.145	Nath and Thingbaijam (2012) 0.15	Sitharam *et al*. (2014) 0.13	Giardini *et al.* (1999) 0.10
Darjeeling	0.42	Nath and Thingbaijam (2012) 0.35	Sitharam *et al*. (2014) 0.3-0.35	Giardini *et al.* (1999) 0.3
Durgapur	0.16	Nath and Thingbaijam (2012) 0.12	Sitharam *et al*. (2014) 0.10-0.15	Giardini *et al.* (1999) 0.05-0.06
Haldia	0.13	Nath and Thingbaijam (2012) 0.12	Sitharam *et al*. (2014) 0.05-0.10	Mohanty and Walling (2008) 0.19 Giardini *et al.* (1999) 0.07-0.08
Malda	0.25	Nath and Thingbaijam (2012) 0.20	Sitharam *et al*. (2014) 0.15-0.20	Giardini *et al.* (1999) 0.16-0.20
Kharagpur	0.11	Nath and Thingbaijam (2012) 0.08	Sitharam *et al*. (2014) 0.05-0.10	Giardini *et al.* (1999) 0.04-0.05
Siliguri	0.33	Nath and Thingbaijam (2012) 0.30	Sitharam *et al*. (2014) 0.30-0.35	Giardini *et al.* (1999) 0.20-0.25

4.5 Probabilistic Seismic Hazard Assessment of Kolkata at Engineering Bedrock

The same protocol of Probabilistic Seismic Hazard Assessment has been adopted for Kolkata as well. Figure 4.18 depicts seismic hazard curves for selected landmarks of Kolkata corresponding to PGA, PSA at 0.2 sec and 1.0 sec respectively at engineering bedrock. Both 2% and 10% Probability of exceedance in 50 years have been demarcated by dotted lines.

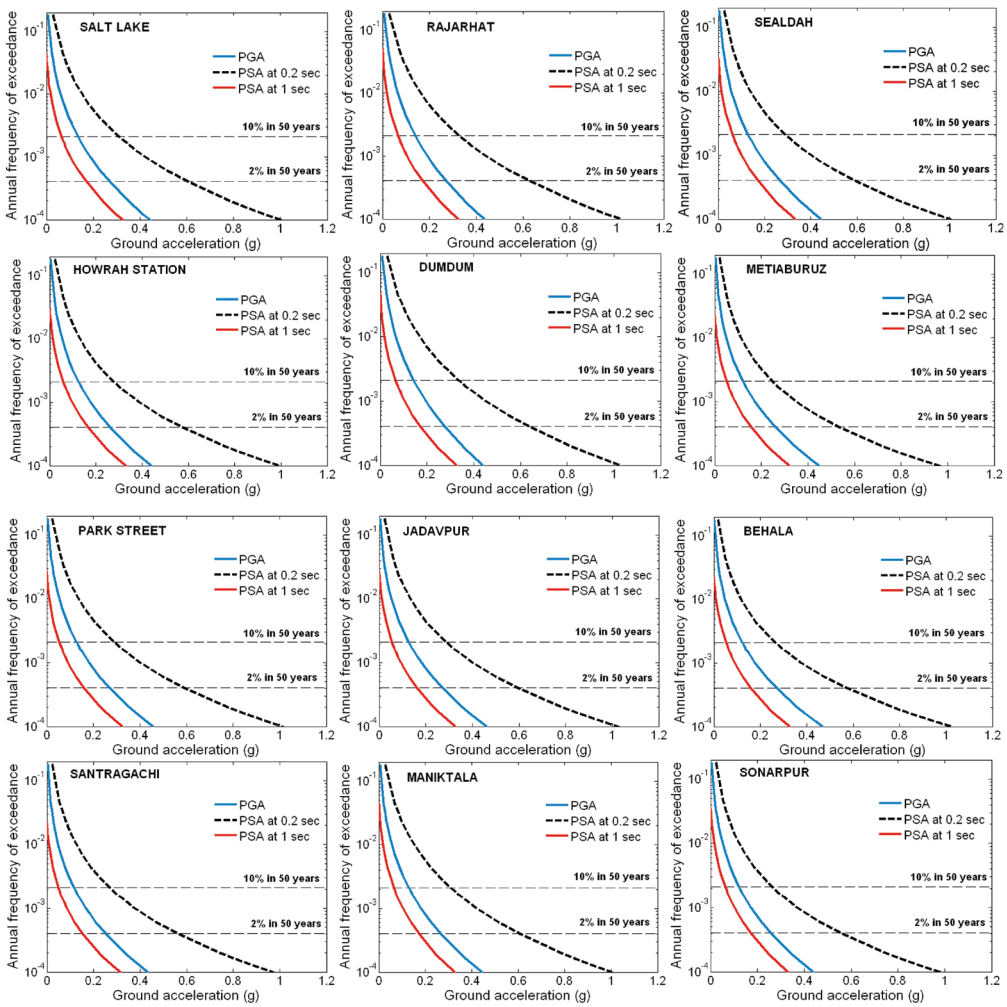

Figure 4.18 **Annual frequency of exceedence vs. Ground Acceleration plots usually termed as Seismic Hazard curves for a few selected locations in Kolkata for Peak and Spectral Accelerations at 0.2 sec and 1.0 sec for uniform firm rock site condition (compliant with $V_s^{30} \sim$ 760 m/s). Both the 10% and 2% probabilities of exceedance in 50 years have been marked by horizontal dotted lines in each plot.**

The PGA distribution in Kolkata shown in Figure 4.19 for 2% probability of exceedance in 50 years varies from 0.24g to 0.28g. The estimated maximum PGA of 0.28g is associated with northeastern part of the City which covers north of Dum Dum Airport, Rajarhat and New Town area. Regions in and around Saltlake also exhibits relatively higher hazard level. The spatial distribution of PSA at both short period 0.2 sec and long period 1.0 sec in Kolkata for 2% probability in 50 years have been depicted in Figure 4.20.

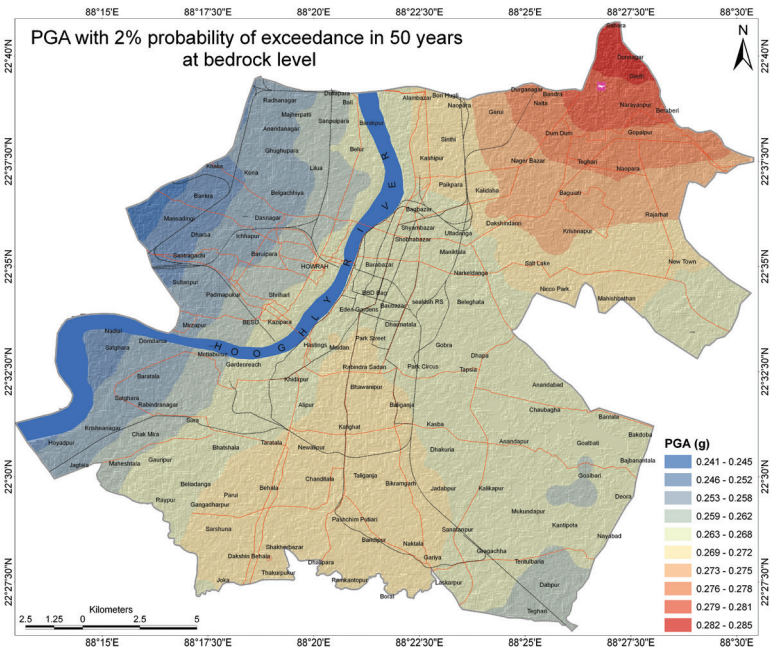

Figure 4.19 **Spatial distribution of PGA in Kolkata with 2% probability of exceedance in 50 years at bedrock.**

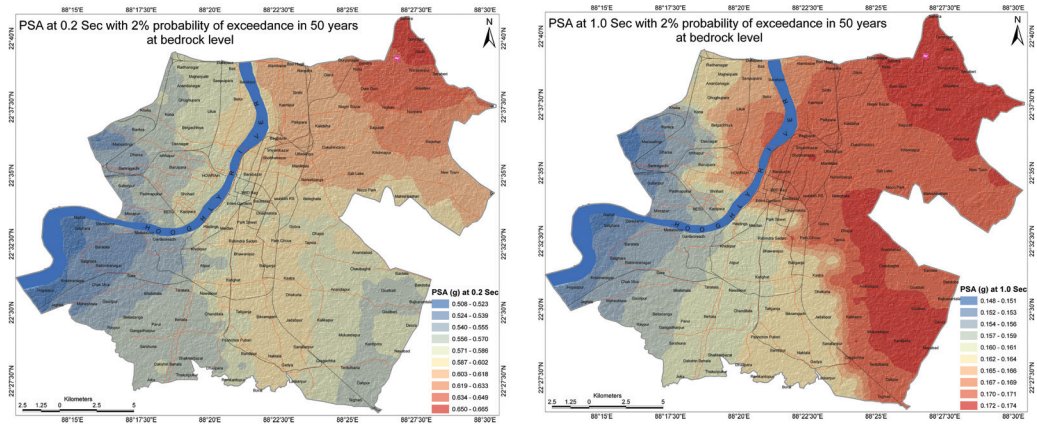

Figure 4.20 **Seismic hazard distribution maps of Kolkata in terms of PSA at 0.2 sec and 1.0 sec for 2% probability of exceedance in 50 years at firm rock site condition.**

The PGA distribution for 10% probability of exceedance in 50 years varies from 0.109g to 0.151g as depicted in Figure 4.21. The regions of Rajarhat, New Town and Saltlake are seen with higher hazard level, while moderate hazard level is associated with the regions of Park Circus, Dhakuria, Kasba, Barabazar and Dharmatala. Low hazard level of around 0.11-0.121g is observed in the southwestern part of Kolkata encompassing areas of Behala, Metiabruz and Mahestala. The region encompassing Dum Dum, Rajarhat, New Town and Saltlake are seen to be associated with PGA range of 0.139-0.151g. The PSA distribution at both short period 0.2 sec and long period 1.0 sec have been depicted in Figure 4.22. The PSA at 0.2 sec exhibits a variation between 0.230g to 0.357g while for 1.0 sec it ranges from 0.047g to 0.069g.

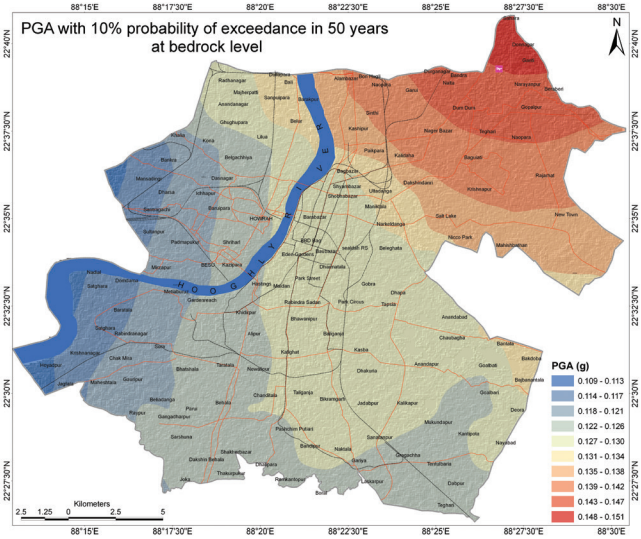

Figure 4.21 **Spatial distribution of PGA in Kolkata with 10% probability of exceedance in 50 years at bedrock.**

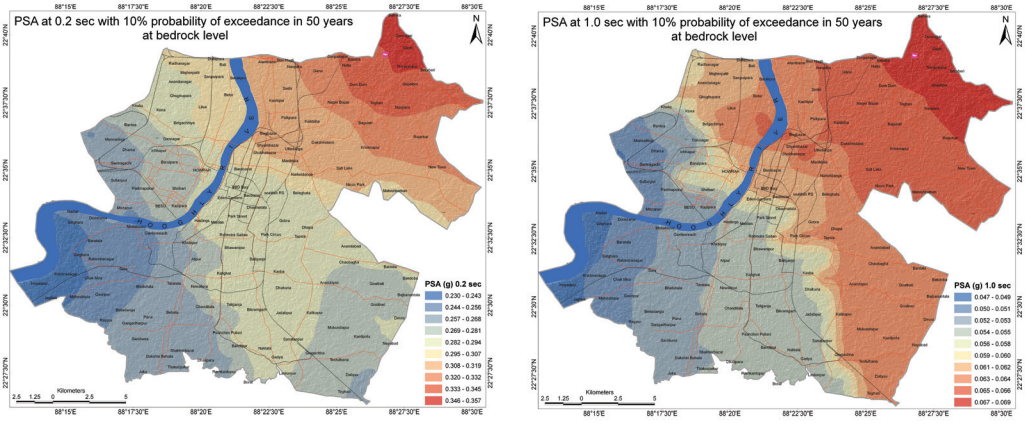

Figure 4.22 **Spatial distribution of PSA at 0.2 sec and 1.0 sec in Kolkata with 10% probability of exceedance in 50 years at bedrock.**

The associated statistical error distribution in terms of ±standard deviation in the predicted PGA and PSA distributions is depicted in Figure 4.23.

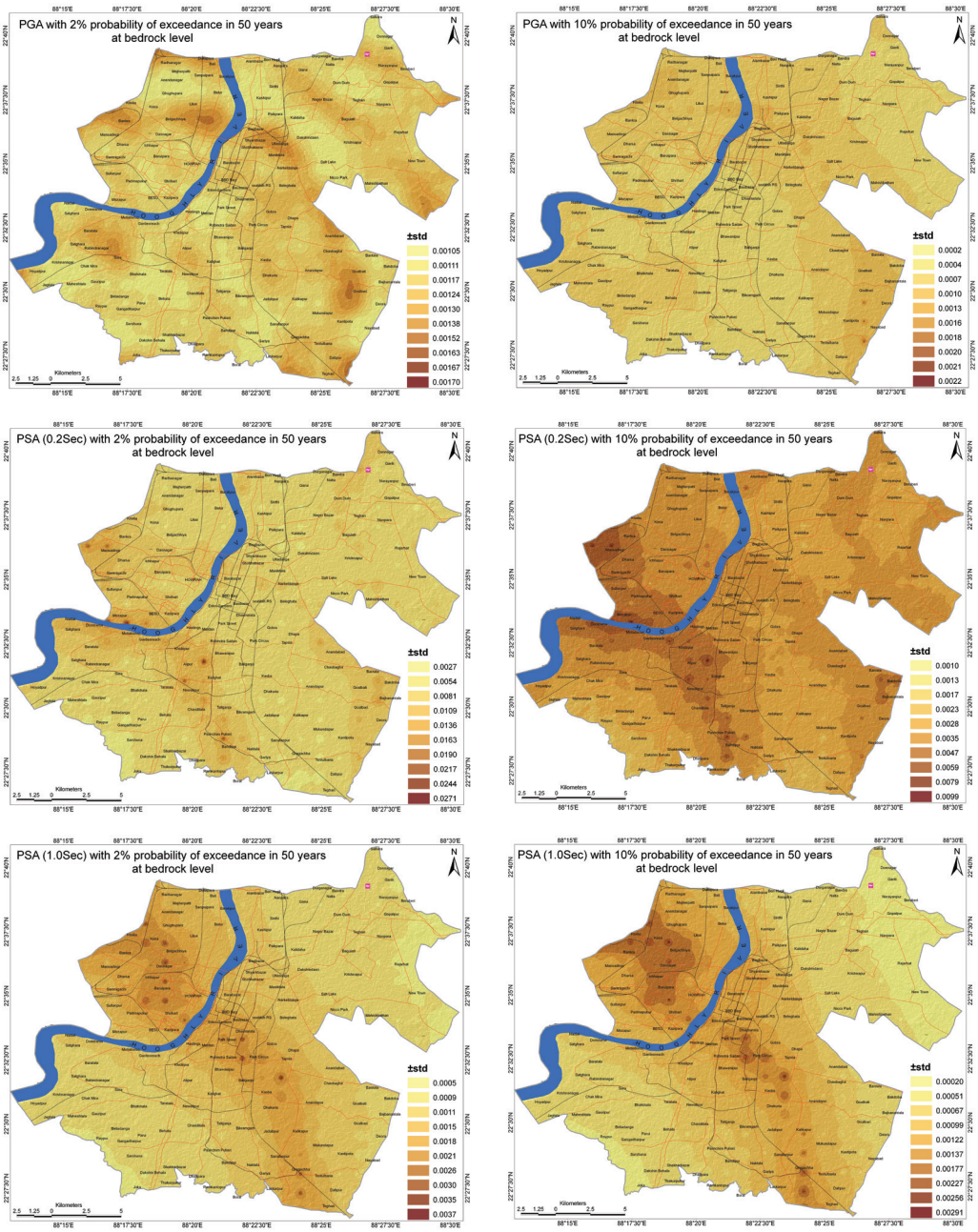

Figure 4.23 **The standard deviation (±σ) spatial distribution associated with PSHA of Kolkata at both 2% and 10% Probability of exceedance in 50 years.**

4.6 Concluding Remarks

The Seismic hazard analysis has emerged as an important issue in high risk urban centers across the globe and is considered an integral part of earthquake induced disaster mitigation practices as PSHA provides useful solutions for end users, mainly as input to seismic design. This study delivers a next generation probabilistic seismic hazard model of West Bengal as well as for Kolkata with the incorporation of different seismic hazard components namely the seismogenic source models, seismicity analysis and ground motion prediction equations in a logic tree framework. The results presented here indicate that the hazard distributions are significantly higher than that specified in the earlier works of GSHAP and BIS (2002). The differences in the estimated hazard distribution compared to the previous studies can be attributed to several factors such as (a) inclusion of NGAs developed in this study and also the employment of multiple GMPEs as appropriate for similar seismotectonic regimes globally which were not included in the earlier studies, (b) Layered seismogenic source framework considerations and smoothed-gridded seismicity models conforming to the variation of seismotectonic attributes with hypocentral depth, (c) depth-wise active fault specific source classification apart from the already considered layered polygonal sources, and (d) multiple models of activity rates for both the layered polygonal and tectonic sources based on intensive seismicity analysis. The present study will facilitate updating the national building-code for earthquake resistant design and construction practices in West Bengal along with the capital city of Kolkata. The assessment of probabilistic seismic hazard adopted in the present analysis is considered as the first and fundamental step towards mitigation process, which inherently reduces the disastrous economic and social effects of earthquakes.